Excitation energies with time-dependent density matrix functional theory: Singlet two-electron systems

Giesbertz, K.J.H.; Pernal, K.; Gritsenko, O.V.; Baerends, E.J.

published in
Journal of Chemical Physics
2009

DOI (link to publisher)
10.1063/1.3079821

document version
Publisher's PDF, also known as Version of record

Excitation energies with time-dependent density matrix functional theory: Singlet two-electron systems

K. J. H. Giesbertz,[1] K. Pernal,[1,2] O. V. Gritsenko,[1] and E. J. Baerends[1,a)]
[1]*Theoretical Chemistry, VU University, De Boelelaan 1083, 1081 HV Amsterdam, The Netherlands*
[2]*Institute of Physics, Technical University of Lodz, ul. Wolczanska 219, 93-005 Lodz, Poland*

(Received 3 November 2008; accepted 20 January 2009; published online 19 March 2009)

Time-dependent density functional theory in its current adiabatic implementations exhibits three striking failures: (a) Totally wrong behavior of the excited state surface along a bond-breaking coordinate, (b) lack of doubly excited configurations, affecting again excited state surfaces, and (c) much too low charge transfer excitation energies. We address these problems with time-dependent density *matrix* functional theory (TDDMFT). For two-electron systems the exact exchange-correlation functional is known in DMFT, hence exact response equations can be formulated. This affords a study of the performance of TDDMFT in the TDDFT failure cases mentioned (which are all strikingly exhibited by prototype two-electron systems such as dissociating H_2 and HeH^+). At the same time, adiabatic approximations, which will eventually be necessary, can be tested without being obscured by approximations in the functional. We find the following: (a) In the fully nonadiabatic (ω-dependent, exact) formulation of linear response TDDMFT, it can be shown that linear response (LR)-TDDMFT is able to provide exact excitation energies, in particular, the first order (linear response) formulation does not prohibit the correct representation of doubly excited states; (b) within previously formulated simple adiabatic approximations the bonding-to-antibonding excited state surface as well as charge transfer excitations are described without problems, but not the double excitations; (c) an adiabatic approximation is formulated in which also the double excitations are fully accounted for. © *2009 American Institute of Physics*.
[DOI: 10.1063/1.3079821]

I. INTRODUCTION

Dissociation of molecular systems poses a serious challenge within the density functional theory (DFT) framework. This is already true for the ground state energy curve, cf. e.g., Refs. 1 and 2. For excited states the problems are even worse, there are various kinds of excitations which are not correctly represented in time-dependent DFT (TDDFT) calculations. Figure 1 displays the failure of TDDFT [in its adiabatic GGA (BP86) variant] for the potential energy surface (PES) of the first excited state of H_2, $1\,^1\Sigma_u^+$. As highlighted in Ref. 3, this PES goes to zero instead of going through a minimum and then asymptotically to ~10 eV as is the case for the exact excitation energy [triple zeta basis plus polarization function (TZP) basis set is used here]. In Ref. 4 this catastrophic behavior of adiabatic TDDFT has also been shown for Li_2 and N_2. B3LYP does not improve the situation the least. This state corresponds to the simple $\sigma_g \rightarrow \sigma_u$ orbital excitation in H_2. The prototypical photochemical bond-breaking event resulting from bonding-to-antibonding orbital excitation takes place on the triplet surface ($1\,^3\Sigma_u^+$) corresponding to the same excited $(\sigma_g)^1(\sigma_u)^1$ configuration. The triplet state is typically populated by intersystem crossing from the singlet state, hence the great importance of this type of excitation. The failure of TDDFT is not just quantitative, in very large basis sets such as aug-cc-pVQZ basis the exact excitation energies as well as the TDDFT ones change considerably for the higher excited states, actually deteriorating the agreement between the two, but the TDDFT $1\,^1\Sigma_u^+$ continues to exhibit the same qualitatively wrong behavior. In Fig. 2 we show the TDDFT Σ_g^+ excitation energies of dissociating H_2. It is evident that there is an exact state (the third at $R_e = 1.4$ bohr), which is completely missing in the TDDFT calculations. It becomes lower with increasing R and has (in the exact calculations) avoided crossings with the second and

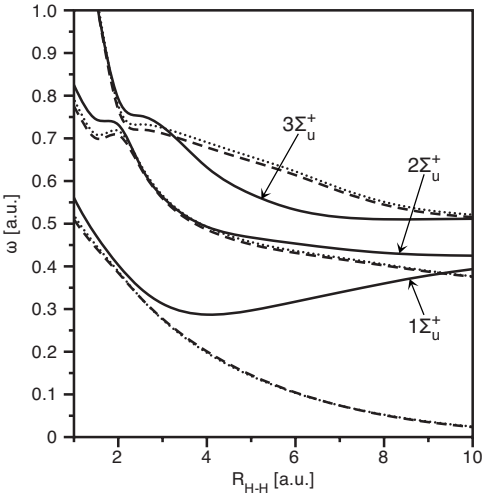

FIG. 1. TDDFT potential energy curves for the lowest $^1\Sigma_u^+$ excited states for dissociating H_2 in a TZP basis set. Solid lines: Exact solutions in the given basis; dashed lines: TDDFT-BP86; dotted lines: TDDFT-B3LYP.

a)Electronic mail: baerends@chem.vu.nl.

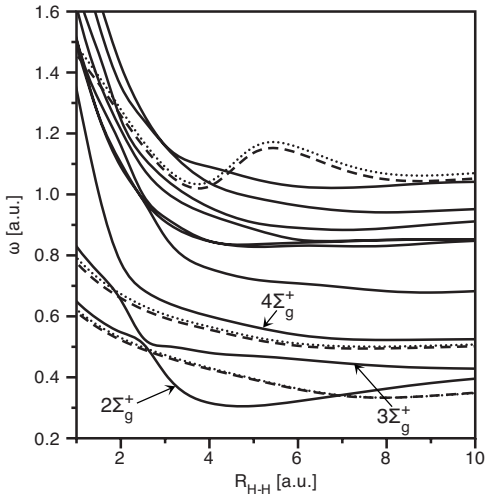

FIG. 2. TDDFT potential energy curves of the lowest $^1\Sigma_g^+$ excited states for dissociating H_2 in a TZP basis. Solid lines: Exact solutions in the given basis; dashed lines: TDDFT-BP86; dotted lines: TDDFT-B3LYP.

first state, becoming the lowest excited $^1\Sigma_g^+$ state ($2\,^1\Sigma_g^+$) from ~2.5 bohr onward. This is a doubly excited state, $(\sigma_g)^2 \rightarrow (\sigma_u)^2$. It is totally missing in the TDDFT calculations. After some initial optimism that such doubly excited states would be accurately calculated in TDDFT,[5–7] it has become clear this is not the case.[8–11] We note in passing that also in the higher part of the spectrum—above 0.6 Hartree—TDDFT performs very poorly, there is hardly any agreement with the exact spectrum. In Fig. 3 the energies for a few charge transfer excitations are shown, namely, the excitation energies for the lowest three $^1\Sigma$ excited states of HeH^+ along the dissociation coordinate. The TDDFT excitation energies exhibit the well-known severe underestimation at long distance, where these excitations have strong charge transfer character, from He($1s$) to H($1s$) in $2\,^1\Sigma$ and from He($1s$) to H($2s,2p_z$) in $3\,^1\Sigma$ and $4\,^1\Sigma$. The hybrid functional B3LYP improves a little on the pure GGA BP86. We note that in the charge transfer excited states we do not have oppositely

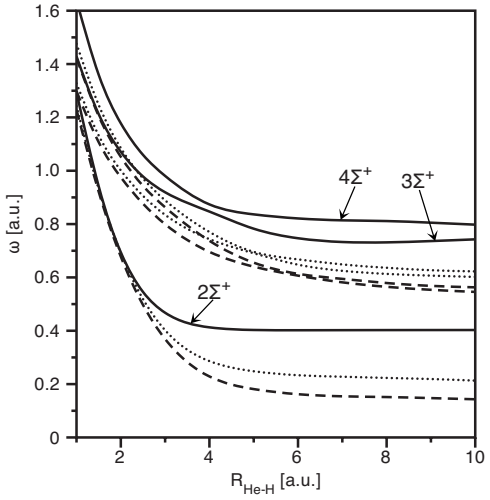

FIG. 3. Potential energy curves of $^1\Sigma$ excitations for dissociating HeH^+. Solid lines: Exact solutions in the given basis; dashed lines: TDDFT-BP86; dotted lines: TDDFT-B3LYP. The dots indicate a high $(1\sigma_g)^2 \rightarrow (1\sigma_u)^2$ double excitation character.

charged fragments, but a neutral atom (H) and a positive ion (He^+). Accordingly, the energy does not have a $-1/R$ asymptotic behavior. One of the errors of TDDFT is that this $-1/R$ behavior is lacking for the case of a positive and negative fragment, but most of the TDDFT error arises from the failure of the adiabatic exchange-correlation kernels of TDDFT to make the large correction that is required in this case[12] to the Kohn–Sham (KS) one-electron energy difference, which is the leading term in the TDDFT excitation energy calculation. We will use the HeH^+ system to test if the methods developed in this paper work for charge transfer excitations, although we recognize that the TDDFT error for he HeH^+ system is somewhat atypical for TDDFT, which we briefly explain in Appendix A.

A remedy for these deficiencies of DFT might be sought in density *matrix* functional theory (DMFT).[13–24] For the ground state total energy curve along the dissociation coordinate, successes have already been reported[18] with approximate DM functionals that represent improvements on the form formulated long ago by Müller[13] and Buijse and co-worker.[14,15] It is the purpose of the present paper to address the above-mentioned problem cases for TDDFT excitation energy calculation with DMFT, using the development of linear response based time-dependent density matrix functional theory.[25,26] We will restrict ourselves to the two-electron systems H_2 and HeH^+, which exhibit all the problems, but which have the advantage that we do not have to introduce an approximate functional since the exact one is known for two-electron systems (see below). A preliminary account has appeared.[27]

We will first set up and study the equations of *exact* linear response (LR)-TDDMFT, without any further approximation, neither an adiabatic approximation (AA) in the "kernel" nor an approximation in the functional. Next we will investigate AAs, which will be advantageous in order to speed up the calculations and which will be required when approximate functionals will be introduced for many-electron systems. Here we shall investigate if adiabatic TDDMFT is able to solve the trouble described above with adiabatic TDDFT.

In DMFT, the one-body reduced density matrix, instead of just the density ($\rho(\boldsymbol{x})$), is used to represent the system. The one-body reduced density matrix of an N-electron system, which will be denoted one-matrix hereafter, is given as

$$\begin{aligned}\gamma(\boldsymbol{x}_1,\boldsymbol{x}_1') &\equiv \langle\Psi|\hat{\psi}^\dagger(\boldsymbol{x}_1')\hat{\psi}(\boldsymbol{x}_1)|\Psi\rangle \\ &= N\int \mathrm{d}\boldsymbol{x}_2 \ldots \int \mathrm{d}\boldsymbol{x}_N \Psi(\boldsymbol{x}_1,\boldsymbol{x}_2,\ldots\boldsymbol{x}_N) \\ &\quad \times \Psi^*(\boldsymbol{x}_1',\boldsymbol{x}_2,\ldots,\boldsymbol{x}_N), \end{aligned} \tag{1}$$

where $\boldsymbol{x}_i$ denotes the combined spatial coordinate and spin index ($\boldsymbol{x}_i = \boldsymbol{r}_i s_i$). Note that the density of the system is given by the diagonal ($\rho(\boldsymbol{x}) = \gamma(\boldsymbol{x},\boldsymbol{x})$). The one-matrix is a Hermitian function, so it can be written in its spectral form

$$\gamma(\boldsymbol{x},\boldsymbol{x}') = \sum_k n_k \chi_k(\boldsymbol{x})\chi_k^*(\boldsymbol{x}'). \tag{2}$$

The eigenfunctions are referred to as natural orbitals (NOs) and the eigenvalues are called the (natural) occupation numbers. If the one matrix is known, the kinetic energy and potential energy of the system are known exactly since they only involve one-body operators. However, the contribution of the interaction between the particles requires knowledge of (the diagonal of) the two-body reduced density matrix, which will be named two-matrix hereafter. We define the two-matrix with the following normalization:

$$\Gamma(\boldsymbol{x}_1\boldsymbol{x}_2,\boldsymbol{x}_2'\boldsymbol{x}_1') \equiv \langle\Psi|\hat{\psi}^\dagger(\boldsymbol{x}_1')\hat{\psi}^\dagger(\boldsymbol{x}_2')\hat{\psi}(\boldsymbol{x}_2)\hat{\psi}(\boldsymbol{x}_1)|\Psi\rangle. \tag{3}$$

The Hohenberg–Kohn theorem[28] for the diagonal density can be extended to the one-matrix: There is a one-one correspondence between ground state wave functions and one matrices ($\Psi \leftrightarrow \gamma$).[29] Therefore all the ground state quantities can be regarded as functionals of the one matrix, including the two matrix. The ultimate success of DMFT will depend on finding accurate one-matrix functionals for the exchange and correlation energies. For two-electron systems, however, such an approximation is not necessary, as can be seen as follows. The spatial part of a singlet two-electron wave function is symmetric at all times t, so the matrix $\boldsymbol{C}(t)$ of Eq. (4) is symmetric as well. It can be diagonalized by a unitary matrix $\boldsymbol{U}(t)$ by the transformation $(\boldsymbol{U}(t)\boldsymbol{C}(t)\boldsymbol{U}^T(t))_{kl}=\boldsymbol{c}_k(t)\delta_{kl}$,

$$\Psi(\boldsymbol{r},\boldsymbol{r}';t) = \sum_{kl} C_{kl}(t)\chi_k(\boldsymbol{r})\chi_l(\boldsymbol{r}') = \sum_k c_k(t)\phi_k(\boldsymbol{r}t)\phi_k(\boldsymbol{r}'t). \tag{4}$$

The density matrix $\boldsymbol{\gamma}=2\boldsymbol{C}\boldsymbol{C}^\dagger$ is obtained in the diagonal form

$$\gamma(\boldsymbol{r},\boldsymbol{r}';t) = \sum_{kl} \gamma_{kl}(t)\chi_k(\boldsymbol{r})\chi_l^*(\boldsymbol{r}') = \sum_k n_k(t)\phi_k(\boldsymbol{r}t)\phi_k^*(\boldsymbol{r}'t), \tag{5}$$

which shows that the wave function coefficients $\boldsymbol{c}(t)$ of Eq. (4) are related to the NO occupation numbers, $n_k(t)=2|c_k(t)|^2$. Also the two-matrix reduces to a particularly simple form

$$\begin{aligned}\Gamma(\boldsymbol{r}_1,\boldsymbol{r}_2,\boldsymbol{r}_2',\boldsymbol{r}_1';t) &= \sum_{klrs} \Gamma_{klrs}(t) \times \chi_s^*(\boldsymbol{r}_1')\chi_r^*(\boldsymbol{r}_2')\chi_l(\boldsymbol{r}_2)\chi_k(\boldsymbol{r}_1) \\ &= \sum_{klrs} [2c_k(t)c_s^*(t)\delta_{kl}\delta_{rs}] \\ &\quad \times \phi_s^*(\boldsymbol{r}_1't)\phi_r^*(\boldsymbol{r}_2't)\phi_l(\boldsymbol{r}_2t)\phi_k(\boldsymbol{r}_1t).\end{aligned} \tag{6}$$

This shows that in a singlet two-electron system the two-matrix can be reconstructed easily from the one-matrix (except that the phase of the expansion coefficients $c_k(t)$ is not known from $\boldsymbol{\gamma}$). It is this property which gives two-electron systems their special place in DMFT.

Lately, it has been realized that analogous to the time-dependent generalization of DFT due to Runge and Gross,[30] a time-dependent formulation of DMFT should also be possible.[25,26] The formalism is based on the equation of motion (EOM) of the one matrix, which depends on the time-dependent two matrix. This equation was already known as a part of the Bogolyubov–Born–Green–Kirkwood–Yvon (BBGKY) hierarchy.[31] The BBGKY hierarchy has a "chain-like" structure, where the calculation of the n-body reduced density matrix requires the EOM of the $(n+1)$-body reduced density matrix. Therefore it contains the EOMs of all the reduced density matrices up to the N-matrix. Using all the reduced density matrices would be equivalent to a calculation of the time-dependent Schrödinger equation and is not feasible. Therefore, this "chain" has to be terminated in actual calculations. It is common practice to retain at least the EOM of the two-matrix to ensure energy conservation.[32] However, in TDDMFT only the EOM of the one matrix is kept and the time-dependent two matrix has to be reconstructed from the time-dependent one matrix, which can be done for singlet two-electron systems.

First we derive in Sec. II some conditions for a stationary state, which serves as our reference state for the linear response. Then we use the time-dependent Schrödinger equation to obtain the EOM for the wave function, in particular, its expansion coefficients $\boldsymbol{C}(t)$. Using the stationary state as a reference state, we derive in Sec. IV exact response equations for the singlet two-electron wave function. Since the wave function and the one matrix have large similarities for the singlet two-electron system, we can easily transform the LR equations of the wave function into exact LR-TDDMFT equations.

Subsequently (Sec. V), these equations are studied. However, the ω-dependence of the effective response matrix in the case of exact LR-TDDMFT precludes finding its zeros by a simple diagonalization. Moreover, the ω-dependence is not known for general N-electron systems. AAs are therefore introduced in Sec. VI. Finally, in Sec. VII the results for the excited state potential energy curves of H_2 and HeH^+ are presented and the conclusions are formulated in Sec. VIII.

II. STATIONARY STATES

The Hamiltonian of a general nonrelativistic two-electron system

$$\hat{H}(\boldsymbol{r}_1,\boldsymbol{r}_2) = \hat{T} + \hat{V} + \hat{W} = \hat{h}(\boldsymbol{r}_1) + \hat{h}(\boldsymbol{r}_2) + w(\boldsymbol{r}_1,\boldsymbol{r}_2), \tag{7}$$

has a one-electron part consisting of the kinetic energy and a local (external) potential

$$\hat{h}(\boldsymbol{r}) = -\tfrac{1}{2}\nabla_{\boldsymbol{r}}^2 + v(\boldsymbol{r}), \tag{8}$$

and a two-particle interaction given by $\hat{W}=w(\boldsymbol{r}_1,\boldsymbol{r}_2)=r_{12}^{-1}$. Since the Hamiltonian is invariant under time-reversal, it suffices to work with a real representation of the wave function for the stationary states. Therefore we can choose all the quantities in the diagonal expansion [Eq. (4)] to be real and we obtain the expression originally noted in Ref. 33,

$$\Psi(\boldsymbol{r}_1,\boldsymbol{r}_2) = \sum_k c_k\chi_k(\boldsymbol{r}_1)\chi_k(\boldsymbol{r}_2). \tag{9}$$

The spatial part of the one-particle density matrix becomes

$$\gamma(\boldsymbol{r},\boldsymbol{r}') = 2\sum_k c_k^2\chi_k(\boldsymbol{r})\chi_k^*(\boldsymbol{r}') \tag{10}$$

so the NO occupations are $n_k=2c_k^2$. Using the following definitions of the integrals:

$$h_{kl} \equiv \int d\boldsymbol{r}\chi_k^*(\boldsymbol{r})\hat{h}(\boldsymbol{r})\chi_l(\boldsymbol{r}), \tag{11a}$$

$$w_{klrs} \equiv \int \mathrm{d}\boldsymbol{r}_1 \int \mathrm{d}\boldsymbol{r}_2 \chi_k^*(\boldsymbol{r}_1)\chi_l^*(\boldsymbol{r}_2)w(\boldsymbol{r}_1,\boldsymbol{r}_2)\chi_r(\boldsymbol{r}_2)\chi_s(\boldsymbol{r}_1), \tag{11b}$$

the energy is simply calculated to be

$$E \equiv \langle\Psi|\hat{H}|\Psi\rangle = \sum_k n_k h_{kk} + \sum_{kl} c_k c_l w_{kkll}. \tag{12}$$

We note in passing that this energy is not strictly a one-matrix functional since it depends on the choice of the signs of the coefficients $\{c_k\}$, while the one matrix, hence any explicit one-matrix functional, does not. This point is not unimportant, but it does not affect the developments in this paper, and we proceed to determine the NOs $\{\chi_k\}$ and coefficients $\{c_k\}$ (and from them the occupations n_k) by optimizing the energy under the constraints that the NOs should be orthonormal and the wave function should be normalized. To this end we introduce the following Lagrangian

$$\Omega = \langle\Psi|\hat{H}|\Psi\rangle - \sum_{kl} \lambda_{kl}(\langle\chi_l|\chi_k\rangle - \delta_{lk}) - \mu\left(\sum_k c_k^2 - 1\right). \tag{13}$$

To optimize the energy under these constraints, we differentiate the Lagrangian Ω with respect to $\chi_l(\boldsymbol{r})$, $\chi_k^*(\boldsymbol{r})$, and c_k to find its stationary points

$$\frac{\delta\Omega}{\delta\chi_k^*(\boldsymbol{r})} = 2\sum_p c_k c_p h_{kp}\chi_p(\boldsymbol{r}) + n_k(\hat{h}\chi_k)(\boldsymbol{r}) + 2\sum_p c_k c_p\langle\chi_k|w|\chi_p\rangle(\boldsymbol{r})\chi_p(\boldsymbol{r}) - \sum_p \lambda_{kp}\chi_p(\boldsymbol{r}) = 0, \tag{14a}$$

$$\frac{\delta\Omega}{\delta\chi_l(\boldsymbol{r})} = 2\sum_p c_p c_l h_{pl}\chi_p^*(\boldsymbol{r}) + n_l(\hat{h}\chi_l)^*(\boldsymbol{r}) + 2\sum_p c_p c_l\langle\chi_p|w|\chi_l\rangle(\boldsymbol{r})\chi_p^*(\boldsymbol{r}) - \sum_p \lambda_{pl}\chi_p^*(\mathbf{r}) = 0, \tag{14b}$$

$$\frac{1}{2}\frac{\partial\Omega}{\partial c_k} = (2h_{kk} - \mu)c_k + \sum_p c_p w_{ppkk} = 0. \tag{14c}$$

The solutions are dependent on the values of the Lagrange multipliers, which we should determine from the constraints. We will, however, not solve the integrodifferential equations for the NOs and the coefficients $\{c_p\}$ explicitly, but derive a few useful relations. Equations (14a) and (14b) determine, with the correct values of the Lagrange multipliers and the coefficients substituted, the NOs. We use the orthogonality constraint by multiplying Eq. (14a) by $\chi_l^*(\boldsymbol{r})$ and multiplying Eq. (14b) by $\chi_k(\boldsymbol{r})$, and integrating to obtain in both cases λ_{kl}. Subtracting these expressions for λ_{kl} gives

$$0 = \int \mathrm{d}\boldsymbol{r}\chi_l^*(\boldsymbol{r})\frac{\delta\Omega}{\delta\chi_k^*(\boldsymbol{r})} - \int \mathrm{d}\boldsymbol{r}\chi_k(\boldsymbol{r})\frac{\delta\Omega}{\delta\chi_l(\boldsymbol{r})} = (n_k - n_l)h_{kl} + 2(c_k - c_l)\sum_p c_p w_{ppkl}, \tag{15}$$

which will be proven useful later.

The Lagrange multiplier μ can be obtained from the normalization constraint by multiplying Eq. (14c) by c_k and summing over k. Using the constraint $\Sigma_k c_k^2 = 1$, one obtains

$$\mu = \sum_k n_k h_{kk} + \sum_{kl} c_k c_l w_{kkll}. \tag{16}$$

Comparing Eq. (16) to Eq. (12), we see that not unexpectedly the energy E and μ (often denoted the chemical potential) are related by $E = \mu$.

Equations (14c) and Eq. (15) can be combined into the simple equation

$$(c_k + c_l)h_{kl} + \sum_p c_p w_{ppkl} = \mu c_k \delta_{kl}, \tag{17}$$

which will be proven to be another useful analytical relation.

Our results in this section constitute sets of equations that determine the stationary wavefunctions. Their solutions are equivalent to the full configuration interaction (CI) solutions. These sets of equations are nonlinear and they are coupled and are difficult to solve in general. We use the results of this section primarily for the analytical relations that have been obtained, in order to simplify the response equations.

III. TIME-DEPENDENT LINEAR RESPONSE DMFT

The excitation energies can be conveniently obtained from the poles of the one-matrix response function $\boldsymbol{\chi}(\omega)$. To obtain $\boldsymbol{\chi}(\omega)$ or to be more precise $\boldsymbol{\chi}^{-1}(\omega)$ we need the equation for the time-dependent response of the one matrix to a small time-dependent perturbing potential, see Ref. 25. For completeness we give a brief derivation here.

We start from the EOM of the one matrix, which can easily be constructed by combining the EOMs of the creation and annihilation operators,

$$i\dot{\gamma}_{kl}(t) = \sum_r (h_{kr}(t)\gamma_{rl}(t) - \gamma_{kr}(t)h_{rl}(t)) + (W_{kl}^\dagger[\gamma](t) - W_{kl}[\gamma](t)), \tag{18}$$

where $\boldsymbol{W}(t)$ is defined as

$$W_{kl}(t) \equiv \sum_{rst} \Gamma_{krst}[\gamma](t)w_{tsrl}. \tag{19}$$

Suppose that the system is first in a stationary state and that the one matrix is given in its diagonal representation $\gamma_{kl} = n_k\delta_{kl}$. Now we perturb the system by a potential $\delta\boldsymbol{v}(t)$. Collecting all first order contributions in the EOM, we have

$$i\delta\dot{\gamma}_{kl}(t) = (n_l - n_k)\delta v_{kl}(t) + \sum_r (h_{kr}\delta\gamma_{rl}(t) - \delta\gamma_{kr}(t)h_{rl}) + \int dt' \sum_{rs} K_{kl,sr}(t-t')\delta\gamma_{rs}(t'), \quad (20)$$

where we used the coupling matrix $\boldsymbol{K}(t-t')$ to describe the effects from the interactions between the electrons

$$K_{kl,sr}(t-t') \equiv \left.\frac{\delta(W^{\dagger}_{kl}[\gamma](t) - W_{kl}[\gamma](t))}{\delta\gamma_{rs}(t')}\right|_{\gamma(0)}. \quad (21)$$

To go to the frequency domain, we take the Fourier transform which conveniently transforms the convolution product in an ordinary product

$$\omega\delta\gamma_{kl}(\omega) = (n_l - n_k)\delta v_{kl}(\omega) + \sum_r (h_{kr}\delta\gamma_{rl}(\omega) - \delta\gamma_{kr}(\omega)h_{rl}) + \sum_{rs} K_{kl,sr}(\omega)\delta\gamma_{rs}(\omega). \quad (22)$$

In general we do not have an explicit expression for $\boldsymbol{K}(\omega)$ and we have to resort to approximations. In particular we will ultimately need ω-independent approximations, which should result from the AA, to make the response equations routinely solvable. However, in this paper we will reconstruct the effects of the exact $\boldsymbol{K}(\omega)$ in the case of a two-electron system by considering the response of the wave function first and transforming it to the response of the one matrix.

IV. WAVE FUNCTION DYNAMICS

The most straightforward way to derive the EOM for the wave function is to use the time-dependent Schrödinger equation directly on a CI expansion for the spatial part of the singlet two-electron wave function

$$i\partial_t \sum_{kl} C_{kl}(t)\chi_k(\boldsymbol{r})\chi_l(\boldsymbol{r}') = \hat{H}(t)\sum_{kl} C_{kl}(t)\chi_k(\boldsymbol{r})\chi_l(\boldsymbol{r}'), \quad (23)$$

as was done in Ref. 26. To obtain an EOM for the expansion coefficients $\boldsymbol{C}(t)$, we multiply by $\chi^*_k(\boldsymbol{r})\chi^*_l(\boldsymbol{r}')$ and integrate over the coordinates to obtain

$$i\dot{C}_{kl}(t) = \sum_r (h_{kr}(t)C_{rl}(t) + C_{kr}(t)h_{rl}(t)) + \sum_{rs} w_{klrs}C_{sr}(t). \quad (24)$$

We will be interested in linear response. Suppose we have a system initially in a stationary state, so $C_{kl}(t) = e^{-iEt}c_k\delta_{kl}$ and Eq. (17) is satisfied. We will perturb the system with a potential $\delta v_{kl}(t)$ which will induce a first order response in the coefficients

$$C_{kl}(t) \to e^{-iEt}(c_k\delta_{kl} + \delta C_{kl}(t)), \quad (25)$$

where for convenience the $\delta C_{kl}(t)$ are defined such that an overall phase factor e^{-iEt} can be used. For the perturbed coefficients $\delta C_{kl}(t)$ we get the following EOM:

$$i\delta\dot{C}_{kl}(t) = (c_l + c_k)\delta v_{kl}(t) - E\delta C_{kl}(t) + \sum_r (h_{kr}(t)\delta C_{rl}(t) + \delta C_{kr}(t)h_{rl}(t)) + \sum_{rs} w_{klrs}\delta C_{sr}(t). \quad (26)$$

In order to exhibit clearly the number of independent variables, we consider separately the response of the real and imaginary parts of the C_{kl},

$$i\delta\dot{C}^{R/I}_{kl}(t) = \delta\tilde{v}^{I/R}_{kl}(t) - \sum_{rs} K_{kl,rs}\delta C^{I/R}_{sr}(t), \quad (27)$$

where we introduced the Hermitian $\boldsymbol{K}$ matrix

$$K_{kl,rs} \equiv E\delta_{ks}\delta_{lr} - (h_{ks}\delta_{lr} + \delta_{ks}h_{lr}) - w_{klrs}, \quad (28a)$$

$$\delta\tilde{v}^{I/R}_{kl}(t) \equiv (c_l + c_k)\delta v^{I/R}_{kl}(t), \quad (28b)$$

$$f^{R/I} \equiv \tfrac{1}{2}[f \pm f^*]. \quad (28c)$$

Because $\boldsymbol{C}$ is a symmetric matrix, there are only m^2+m independent variables [all $\delta C^{I/R}_{kl}(t), l \le k$] and equations. The equations are Fourier transformed to the frequency domain,

$$\omega\delta C^{R/I}_{kl}(\omega) + \sum_{r\le s} \tilde{K}_{kl,rs}\delta C^{I/R}_{sr}(\omega) = \delta\tilde{v}^{I/R}_{kl}(\omega), \quad (29)$$

where $\tilde{\boldsymbol{K}}$ is defined as

$$\tilde{K}_{kl,rs} \equiv \frac{1}{1+\delta_{rs}}[K_{kl,rs} + K_{kl,sr}]. \quad (30)$$

Note that we effectively derived the inverse response function, $\boldsymbol{\chi}^{-1}(\omega)$, for $\delta\boldsymbol{C}$ and $\delta\tilde{\boldsymbol{v}}$. This can be better seen if we cast Eq. (29) in the matrix form

$$\begin{pmatrix} \omega\mathbf{1}_{M+m} & \tilde{\boldsymbol{K}} \\ \tilde{\boldsymbol{K}} & \omega\mathbf{1}_{M+m} \end{pmatrix}\begin{pmatrix} \delta\boldsymbol{C}^R(\omega) \\ \delta\boldsymbol{C}^I(\omega) \end{pmatrix} = \begin{pmatrix} \delta\tilde{\boldsymbol{v}}^I(\omega) \\ \delta\tilde{\boldsymbol{v}}^R(\omega) \end{pmatrix}. \quad (31)$$

The excitation energies are easily found as the eigenvalues of $\tilde{\boldsymbol{K}}$ since we need for an excitation

$$0 = |\boldsymbol{\chi}^{-1}(\omega)| = \begin{vmatrix} \omega\mathbf{1} & \tilde{\boldsymbol{K}} \\ \tilde{\boldsymbol{K}} & \omega\mathbf{1} \end{vmatrix} = |\omega\mathbf{1} - \tilde{\boldsymbol{K}}| \cdot |\omega\mathbf{1} + \tilde{\boldsymbol{K}}|. \quad (32)$$

We use m for the number of diagonal elements $C^{R/I}_{kk}, k = 1,\ldots,m$ (m is the number of basis functions), and $M = m(m-1)/2$ for the number of unique off-diagonal $\boldsymbol{C}^{R/I}$ elements ($\{C^{R/I}_{kl}\}, l<k$). As an illustration we have calculated the excitation energies of H_2 by diagonalizing $\tilde{\boldsymbol{K}}$ in an aug-cc-pVQZ basis set.[34,35] First the ground state NOs were obtained by a CI singles and doubles (CISD) calculation with the GAMESS-U.K. package.[36] The integrals in the NO basis were stored on file for the excitation calculation. The expansion coefficients $\{c_p\}$ were calculated within the program using Eq. (14c) directly. For the linear algebra we used the LAPACK routines.[37]

The results for the first $^1\Sigma^+_g$ and $^1\Sigma^+_u$ excitations are shown in Table I. As a check we also calculated the excitation energies exactly (within the given basis set) by solving for multiple roots in CISD calculations with the DALTON

TABLE I. The first Σ_g^+ and Σ_u^+ excitations of H_2 in hartree for several bond distances compared to a DALTON CISD calculation.

R_{H-H} (bohr)	Excitation	DALTON	Eq. (32)
1.5	Σ_g^+	0.470 341 871	0.470 341 869
	Σ_u^+	0.452 601 361	0.452 601 359
5.0	Σ_g^+	0.294 179 573	0.294 179 573
	Σ_u^+	0.289 329 519	0.289 329 519
10.0	Σ_g^+	0.362 455 118	0.362 455 117
	Σ_u^+	0.362 402 224	0.362 402 224

package.[38] These benchmark values are shown in the first column. For a good agreement it was necessary to set a very tight criterion for the roots in Dalton and explicitly demand a Cartesian basis set (which is what we are also using). The agreement between the CISD (full-CI in this case) and the linear response calculations is perfect (within the numerical precision of the calculations). It is to be noted that the lowest excited $^1\Sigma_g^+$, which we have seen involves doubly excited configurations, is perfectly represented in the linear response calculations.

V. EXACT LINEAR RESPONSE TDDMFT

A. The exact (ω-dependent) equations

We now proceed to derive the exact response equations of the density matrix, $\delta\gamma(\omega)$. Since the one matrix is Hermitian, we have m^2 variables in total (the M real and M imaginary parts of the off-diagonal elements $\delta\gamma_{kl}(\omega)$, $l<k$, and m real diagonal elements). In general the wave function has many more degrees of freedom, but in the two-electron case this is actually only m more (the imaginary parts of the diagonal elements δC_{kk}^I have to be included since the $\boldsymbol{C}$ matrix is symmetric, not Hermitian). The size of the TDDMFT response problem is not only reduced compared to the wave function response of Eq. (29), the structure of the response equations is also more complicated due to ω-dependence of the DM response matrix, see below.

The one matrix is simply related to the wave function expansion coefficients as $\gamma_{kl}(t)=2(\boldsymbol{C}(t)\boldsymbol{C}^\dagger(t))_{kl}$, so for the perturbed $\delta\gamma^{R/I}(\omega)$ we have $\delta\gamma_{kl}^{R/I}(\omega)=2(c_l\pm c_k)\delta C_{kl}^{R/I}(\omega)$ [$(-)$ sign for the imaginary parts]. We see that all the $\delta\boldsymbol{C}(\omega)$ terms have a corresponding $\delta\boldsymbol{\gamma}(\omega)$ term except the diagonal δC_{kk}^I, which agrees exactly with the fact that m fewer variables are needed for the density matrix response.

It is convenient to use instead of the off-diagonal $\delta\gamma_{kl}(\omega)$ the equivalent variables

$$\delta\tilde{\gamma}_{kl}^R(\omega)=\delta\gamma_{kl}^R(\omega)/2(c_l+c_k)=\delta C_{kl}^R(\omega), \tag{33a}$$

$$\delta\tilde{\gamma}_{kl}^I(\omega)=\delta\gamma_{kl}^I(\omega)/2(c_l-c_k)=\delta C_{kl}^I(\omega), \tag{33b}$$

for the elements $l<k$. For the diagonal elements we use instead of $\delta\gamma_{kk}(\omega)=\delta n_\kappa(\omega)$ the variables

$$\delta\tilde{n}_k(\omega)=\delta\gamma_{kk}(\omega)/4c_k=\delta C_{kk}^R(\omega). \tag{33c}$$

We can now immediately use the linear response equations of the wave function to obtain the TDDMFT response equations up to this trivial transformation

$$\left(\omega-\frac{\boldsymbol{C}\boldsymbol{C}^T}{\omega}\right)\delta\tilde{\boldsymbol{\gamma}}^R(\omega)+\boldsymbol{\mathcal{A}}\delta\tilde{\boldsymbol{\gamma}}^I(\omega)-\frac{\boldsymbol{C}\boldsymbol{\mathcal{E}}}{\omega}\delta\tilde{\boldsymbol{n}}(\omega)$$

$$=-\frac{1}{\omega}\boldsymbol{C}\delta\tilde{\boldsymbol{v}}^D(\omega), \tag{34a}$$

$$\omega\delta\tilde{\boldsymbol{\gamma}}^I(\omega)+\boldsymbol{\mathcal{A}}\delta\tilde{\boldsymbol{\gamma}}^R(\omega)+\boldsymbol{C}\delta\tilde{\boldsymbol{n}}(\omega)=\delta\tilde{\boldsymbol{v}}^R(\omega), \tag{34b}$$

$$\left(\omega-\frac{\boldsymbol{\mathcal{E}}^2}{\omega}\right)\delta\tilde{\boldsymbol{n}}(\omega)+\boldsymbol{C}^T\delta\tilde{\boldsymbol{\gamma}}^I(\omega)-\frac{\boldsymbol{\mathcal{E}}\boldsymbol{C}^T}{\omega}\delta\tilde{\boldsymbol{\gamma}}^R(\omega)$$

$$=-\frac{1}{\omega}\boldsymbol{\mathcal{E}}\delta\tilde{\boldsymbol{v}}^D(\omega), \tag{34c}$$

where we denoted the off-diagonal subblock of $\tilde{\boldsymbol{K}}$ with $\boldsymbol{\mathcal{A}}$, the diagonal subblock with $\boldsymbol{\mathcal{E}}$ and the off-diagonal $\times$diagonal subblock with $\boldsymbol{C}$, i.e.,

$$\mathcal{A}_{kl,sr}=\tilde{K}_{kl,rs}\ \forall\ k\neq l,\quad r\neq s, \tag{35a}$$

$$=E(\delta_{kr}\delta_{ls}+\delta_{ks}\delta_{lr})-(w_{klsr}+w_{klrs})$$
$$-(\delta_{kr}h_{ls}+\delta_{ks}h_{lr}+\delta_{lr}h_{ks}+\delta_{ls}h_{kr}), \tag{35b}$$

$$\mathcal{C}_{kl,r}=\tilde{K}_{kl,rr}\ \forall\ k\neq l, \tag{35c}$$

$$=-2(h_{kl}(\delta_{kr}+\delta_{lr})+w_{klrr}), \tag{35d}$$

$$\mathcal{E}_{kr}=\tilde{K}_{kk,rr}=2((E-2h_{kk})\delta_{kr}-w_{kkrr}). \tag{35e}$$

For the potential $\delta\tilde{\boldsymbol{v}}$ we write $\delta\tilde{\boldsymbol{v}}^D$ for the vector of diagonal elements $\delta\tilde{\boldsymbol{v}}_{kk}, k=1,\ldots,m$, while $\delta\tilde{\boldsymbol{v}}^R$ is the vector of off-diagonal elements $\delta\tilde{v}_{kl}, k>l$. The matrices $\boldsymbol{\mathcal{A}}$ and $\boldsymbol{\mathcal{E}}$ are Hermitian, while $\boldsymbol{C}$ is symmetrical in the kl indices in the case of real functions.

Note that these equations are exact response equations for the one matrix. They show the explicit ω-dependence of the nonadiabatic terms in the response equations, which is

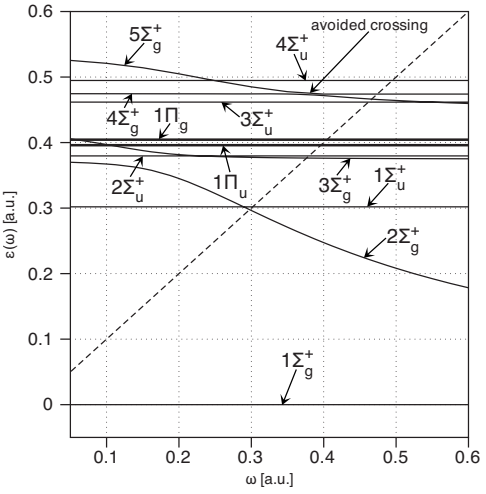

FIG. 4. The eigenvalues $\epsilon_i(\omega)$ of $(\omega\mathbf{1}-\boldsymbol{\chi}(\omega))^{-1}$ for H_2 at a bond distance of 5.0 bohr calculated with an aug-cc-pVQZ basis set, plotted as function of ω. To speed up the calculation, only pairs kl with $l\leq 3$ and $k=1,\ldots,m$ were used (see Sec. V C). The thick lines are doubly degenerate roots. The dashed line is $\epsilon(\omega)=\omega$.

TABLE II. Most important components of the Σ_g^+ excitations of H_2 at $R(H-H)=5.0$ bohr.

	$1\Sigma_g^+$	$2\Sigma_g^+$	$3\Sigma_g^+$	$4\Sigma_g^+$	$5\Sigma_g^+$
k,l			$\lvert\delta\tilde{\gamma}_{kl}^R\rvert^2+\lvert\delta\gamma_{kl}^I\rvert^2$		
3,1			0.18	0.13	0.14
6,1		0.18		0.03	0.09
19,2		0.04	0.15	0.13	0.10
109,1		0.07	0.28	0.42	0.03
110,2			0.04		0.33
k			$\lvert\delta\tilde{n}_k\rvert^2$		
1	0.63	0.19		0.02	
2	0.37	0.33	0.01	0.04	

pleasingly simple. Further note that these equations are nonlinear in ω which implies that the excitation energies cannot be calculated by a straightforward diagonalization. Instead, we have to solve the following matrix equation:

$$\begin{pmatrix} \frac{\mathcal{C}\mathcal{C}^T}{\omega} & -\mathcal{A} & \frac{\mathcal{C}\mathcal{E}}{\omega} \\ -\mathcal{A} & 0 & -\mathcal{C} \\ \frac{\mathcal{E}\mathcal{C}^T}{\omega} & -\mathcal{C}^T & \frac{\mathcal{E}^2}{\omega} \end{pmatrix} \begin{pmatrix} \delta\tilde{\boldsymbol{\gamma}}^R(\omega) \\ \delta\tilde{\boldsymbol{\gamma}}^I(\omega) \\ \delta\tilde{\boldsymbol{n}}(\omega) \end{pmatrix} = \omega \begin{pmatrix} \delta\tilde{\boldsymbol{\gamma}}^R(\omega) \\ \delta\tilde{\boldsymbol{\gamma}}^I(\omega) \\ \delta\tilde{\boldsymbol{n}}(\omega) \end{pmatrix}. \quad (36)$$

We can solve the equations iteratively by diagonalizing the matrix for trial values of ω, and search for those values of ω, where an eigenvalue $\epsilon_i(\omega)$ becomes equal to the input ω. The solutions are the ω values where the curve $\epsilon_i(\omega)$ intersects the line $\epsilon=\omega$. As an example of this procedure we show the lowest roots $\epsilon_i(\omega)$ of the matrix as a function of ω in Fig. 4 and determine its intersections with $\epsilon=\omega$. It is interesting that we have here an example of the form the ω-dependence of the exchange-correlation kernel may take, and of the effects of this ω-dependence, which has received considerable attention in the TDDFT case.[8,9,39,40] For all ω there is an $\epsilon_0(\omega)=0$ eigenvalue. The line $\epsilon_0(\omega)=0$ is cut by the $\epsilon=\omega$ line at $\omega=0$, yielding the trivial "zero-excitation" solution $\omega=0$ (this solution is better called "trivial" than "erroneous," cf. Ref. 25). We will next discuss the results that are obtained in this way for the excitation energies and for the composition of the solution vectors of $\delta\tilde{\gamma}_{kl}$ elements.

TABLE III. Most important components of the $\Pi_{g/u}$ excitations at $R(H-H)=5.0$ bohr.

	$1\Pi_u$	$1\Pi_g$
k,l	$\lvert\delta\tilde{\gamma}_{kl}^R\rvert^2+\lvert\delta\tilde{\gamma}_{kl}^I\rvert^2$	
4,1+5,1	0.51	
4,2+5,2		0.41
10,1+11,1	0.22	
10,2+11,2		0.15
50,1+51,1		0.32
50,2+51,2	0.14	

TABLE IV. Most important contributions to the Σ_u^+ excitations $R(H-H)=5.0$ bohr.

	$1\Sigma_u^+$	$2\Sigma_u^+$	$3\Sigma_u^+$	$4\Sigma_u^+$
k,l		$\lvert\delta\tilde{\gamma}_{kl}^R\rvert^2+\lvert\delta\tilde{\gamma}_{kl}^I\rvert^2$		
2,1	0.68	0.02		0.12
3,2	0.04	0.08	0.18	0.11
19,1	0.08	0.27		0.11
109,2		0.12	0.18	0.38
110,1		0.16	0.37	

B. Interpretation of the results of TDDMFT calculations

The following observations can be made (see the composition of the solution vectors in Tables II–IV and NO composition in Table V).

(a) The most striking observation is that many excitation energies are totally independent of ω, and are equal to the exact energies at any ω. This is strong encouragement for TDDMFT. For the present highly symmetrical molecule this phenomenon is related to the symmetry, i.e., all excitations to states of different symmetries than the ground state, e.g., to Σ_u^+, Π_u, and Π_g states, are independent of ω. Good quality will certainly persist with (small) perturbation of the symmetry (see below for HeH^+). This indicates that ω-dependence is relatively unimportant, which suggests that very accurate excitation energies can also be obtained within AAs (ω-independent approximations) to the inverse response matrix of TDDMFT. The distinguishing electronic structure feature of these excitations is that they do not contain diagonal doubles (no $\delta\tilde{\boldsymbol{n}}$ elements): Simultaneous double excitations to the same orbital occur in a different symmetry (Σ_g^+). Table IV demonstrates that the $1\,{}^1\Sigma_u^+$ at 5 bohr is predominantly the $1\sigma_g \rightarrow 1\sigma_u$ single excitation, as expected. (All our calculations are for singlet excited states; we will not indicate this explicitly in the state symbols.) Similarly the lowest Π_u and Π_g excitations have the expected character of single excitation to the $2p_\pi$ orbitals. The higher excitations in these symmetries also have plausible electronic character. However, the NOs are ordered by their occupation numbers. There are no orbital energies like in the KS model. Low occupation numbers sometimes

TABLE V. Most important atomic orbital (AO) contributions to the NOs.

NO	Irreducible representation	Main AO
1	σ_g	$1s$
2	σ_u	$1s$
3	σ_g	$2p_z$
4/5	π_u	$2p_x/2p_y$
6	σ_g	Hybrid
10/11	π_u	$3d_{xz}/3d_{yz}$
19	σ_u	$2p_z$
50/51	π_g	$2p_x/2p_y$
109	σ_g	$2s$
110	σ_u	$2s$

correspond to energetically easily accessible states.

(b) With respect to the Σ_g^+ states it is very interesting to observe that the double excitations, notably to the $2\Sigma_g^+$ state with much $(1\sigma_g)^2 \rightarrow (1\sigma_u)^2$ character, are also given exactly in the LR-TDDMFT calculations, dependent, however, on the proper treatment of the ω-dependence. The $\omega=0$ root occurs in this symmetry, it corresponds to the ground state $1\Sigma_g^+$ and yields precisely the composition of the ground state in terms of the $(1\sigma_g)^2$ and $(1\sigma_u)^2$ configurations. The linear response formalism does not pose any problem for double excitations. This is a significant difference between density matrix response equations and density response equations, which are employed in TDDFT. Double excitations can naturally be represented in TDDMFT with the $\delta\tilde{n}_k$ terms ("diagonal doubles") and with $\delta\tilde{\gamma}^R_{kl}$, $k>l$, k and l both virtual ("off-diagonal doubles"), while in TDDFT only occupied-virtual orbital products ("single excitations") feature. It is in principle possible to obtain correct excitation energies corresponding to double excitations also in TDDFT, but then the AA has to be abandoned.[8,9,41] Interestingly, we see in Fig. 4 that in the exact TDDMFT calculations it is the $2\Sigma_g^+$, corresponding to the doubly excited configuration $(1\sigma_u)^2$, that exhibits significant ω-dependence. Therefore, one might expect that such double excitations are much harder to treat within an AA in TDDMFT too (but see below). We observe that it is not the double excitation nature per se that is the problem. Off-diagonal doubles which yield states of different symmetry than the ground state [e.g., the $(1\sigma_u)^1(1\pi_u)^1$ configuration leading to a Π_g state], do yield exact excitation energies at any ω. It is also not just a matter of symmetry, i.e., not all states of the same symmetry as the ground state are problematic. For instance, the $3\Sigma_g^+$ is very flat around the excitation energy $\omega=0.376$ H, at which $\epsilon_{2\Sigma_g^+}(\omega)=\omega$. At those ω-values it has virtually no diagonal double ($\delta\tilde{n}$) character, and only a modest amount of off-diagonal double excitation character [excitation to NO pair (2,19), see Table II]. It is basically a $\mathrm{H}_a(1s)\cdot\mathrm{H}_b(2s,2p_z)+\mathrm{H}_a(2s,2p_z)\cdot\mathrm{H}_b(1s)$ state (excitations $1\rightarrow 109$ and $1\rightarrow 3$), while the near by $2\Sigma_u^+$ is $\mathrm{H}_a(1s)\cdot\mathrm{H}_b(2s,2p_z)-\mathrm{H}_a(2s,2p_z)\cdot\mathrm{H}_b(1s)$. It is the diagonal doubles, represented by large $\delta\tilde{n}_k$ elements, such as occur in the $2\Sigma_g^+$, which lend a state significant ω-dependence. Interestingly, the $2\Sigma_g^+$ becomes rather flat (ω-independent) at small values of ω, see Fig. 4, and indeed we observed that for $\omega\rightarrow 0$ the $2\Sigma_g^+$ loses its $\delta\tilde{n}$ character (the $3\Sigma_g^+$ acquires some). The $4\Sigma_g^+$ has no $\delta\tilde{n}$ character, and is perfectly flat, until $\omega \approx 3.0$, but then in the avoided crossing with $5\Sigma_g^+$ it takes over the (modest) double excitation character of the latter and is no longer flat.

(c) At any ω-value we diagonalize a $(M+M+m=m^2)$-dimensional matrix and obtain this number of eigenvalues. Yet, the ω-dependence of the matrix, together with the condition $\epsilon_i(\omega)=\omega$ provides for m^2+m roots, the same number (and values) as in the wave function case. This is better illustrated with a simple example, which we will offer for just a two-orbital case ($m=2$) in Appendix A. It can also be easily inferred that Eq. (36) has m^2+m solutions in the following way. Write Eq. (36) in the homogeneous form by moving the right hand side to the left hand side, i.e., adding $-\omega$ to the diagonal of the matrix in the lhs. Solutions to the homogeneous set of equations are obtained if the determinant of the matrix is zero. It is elementary to show that the characteristic polynomial in ω that is obtained is of order m^2+m, hence m^2+m roots.

C. Dimensional considerations

At this point we comment on the size of the matrix problems of the linear response TDDMFT equations. We will use AAs in the next sections which will remove the ω-dependence of the matrix to be diagonalized, so we are left with a diagonalization problem of dimension m^2 (or half of that when we can exploit that the roots appear in positive-negative pairs). This is effectively the square of the basis set size, which is (notably in many-electron systems) much smaller than the size of typical CI calculations, certainly than the full-CI problem, but still considerably larger than the size of TDDFT equations (only occupied-virtual orbital products). However, in practice the TDDFT and TDDMFT dimensions will be much more similar since most of the increase in the size of the problem compared to TDDFT comes from the many virtual-virtual elements $\delta\tilde{\gamma}_{kl}, k, l$ both virtuals. These are not all needed, as is suggested by the composition of the solution vectors discussed above, and which can be seen as follows. Let us refer to the strongly occupied NOs ($\chi_p, p\leq N/2, N$ is the number of electrons) as the "occupied orbitals" and to the weakly occupied ones ($\chi_p, p>N/2$) as the "virtual orbitals." With respect to the interpretation of the linear response results, we should caution that the higher NO virtuals (very weakly occupied ones) are totally different compared to Hartree–Fock (HF) or DFT virtuals. On the other hand, the occupied NOs and "lower" virtual NOs (i.e., the still significantly occupied ones) do correspond to the occupied and lower virtual "valence orbitals" of HF or DFT. One would expect that in particular the "higher" (very weakly occupied) virtual-virtual pairs kl will not give a significant contribution to the (lower) excitation energies. On the other hand, in for instance H_2 the $l=2$ orbital $(1\sigma_u)$ can hardly be classified as a virtual orbital at long bond distances, where in the ground state the $(1\sigma_u)^2$ configuration mixes strongly with the $(1\sigma_g)^2$ configuration. Its occupation will tend to 1.0 from below at long bond distance. In view of practical applications it is important to determine to what extent virtual-virtual pairs might be excluded, in order to reduce the dimension of the inverse response matrix ($\boldsymbol{\chi}^{-1}$) and speed up the calculation. As a simple test we have done the excitation calculation with only a limited number of pairs. For this purpose we exploit the fact that in the two-electron system the exact wave function dynamics leads to practically the same size of the problem [cf. Eqs. (31) and (32)] and to the same variables ($\delta\tilde{\gamma}^{R/I}_{kl}=\delta C^{R/I}_{kl}$) as the TDDMFT. We can omit in Eq. (32) selected virtual-virtual pairs

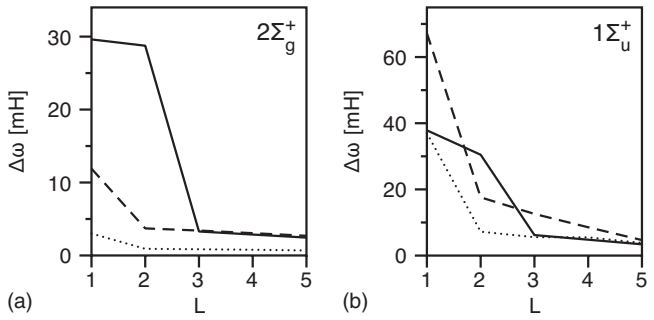

FIG. 5. Plot of the error in the first $^1\Sigma_g^+$ (left) and $^1\Sigma_u^+$ (right) excitations as a function of the maximum l value ($l \leq L$). All k are used in $\delta\tilde{\gamma}_{kl}$ and $\delta\tilde{\gamma}_{kk}$. The straight, dashed, and dotted lines are the excitation energies for bond distances of 1.5, 5.0, and 10.0 bohr, respectively.

and with simple diagonalization (without a tedious search through ω-values) determine how the results are affected compared to the exact benchmark results of Table I.

The results for H_2 are shown in Figs. 5 for the first $^1\Sigma_g^+$ and first $^1\Sigma_u^+$ excitation. All "diagonal" elements $\delta C_{kk}^{R/I}$ are always included. For the off-diagonal elements $\delta\tilde{\gamma}_{kl}^{R/I}, l \leq k-1$, the range of l is restricted, while k runs always over all m NOs. We denote the maximum l value with L, so that in the kl pairs $l \leq \min(k-1, L)$. Restricting l to occupied orbitals only (in this case there is only one occupied orbital, so $L=1$), gives approximately the size of the TDDFT problem. This still yields a sizable error of several hundredths Hartree at the equilibrium distance, which resembles the poorer TDDFT cases. However, the error rapidly drops with addition of just the first and second virtual to the "l set." The errors also generally diminish at larger bond distances of H_2. So restricting l to only the first three highest occupied NOs reproduces the excitation energies quite well already. The matrix to be diagonalized in the aug-cc-pVQZ basis is reduced significantly from a 6105×6105 matrix to a 434×434 matrix, with a large concomitant increase in speed. Thus, the size of the diagonalization problem is not excessively increased compared to TDDFT.

VI. CONNECTIONS WITH ADIABATIC APPROXIMATIONS

A. Relation with the static approximation

It is desirable to develop approximations such that we can obtain (approximate) excitation energies by solving eigenvalue equations without ω-dependence in the matrix. This is usually achieved by AA to the coupling matrix $\boldsymbol{K}(\omega)$ of Eq. (22) whose ω-dependence is not known for general N-electron systems anyway. Here we investigate how, starting from the exact TDDMFT equations [Eq. (34)] and considering their $\omega \to 0$ limit, ω-independent equations may be obtained and how they are related to the AAs studied earlier.[26]

In the $\omega \to 0$ limit, the exact TDDMFT equations should give correct static response equations. It is immediately clear that the $1/\omega$ terms in the exact Eq. (34) will diverge for small ω. In fact for $\omega \to 0$ these terms should perfectly balance each other in both Eqs. (34a) and (34c), to avoid divergence. This yields the following equations:

$$\boldsymbol{\mathcal{C}}(\boldsymbol{\mathcal{C}}^T \delta\tilde{\boldsymbol{\gamma}}^R(0) + \boldsymbol{\mathcal{E}}\,\delta\tilde{\boldsymbol{n}}(0) - \delta\tilde{\boldsymbol{v}}^D(0)) = 0, \tag{37a}$$

$$\boldsymbol{\mathcal{E}}(\boldsymbol{\mathcal{C}}^T \delta\tilde{\boldsymbol{\gamma}}^R(0) + \boldsymbol{\mathcal{E}}\,\delta\tilde{\boldsymbol{n}}(0) - \delta\tilde{\boldsymbol{v}}^D(0)) = 0. \tag{37b}$$

These equations are satisfied if the m-dimensional vector

$$\boldsymbol{\mathcal{C}}^T \delta\tilde{\boldsymbol{\gamma}}^R(0) + \boldsymbol{\mathcal{E}}\,\delta\tilde{\boldsymbol{n}}(0) - \delta\tilde{\boldsymbol{v}}^D(0) \tag{38}$$

belongs to the kernel of both the matrices $\boldsymbol{\mathcal{C}}$ and $\boldsymbol{\mathcal{E}}$. The kernel of both matrices consists of just the vector $\boldsymbol{c}$, as can be seen by multiplying $\boldsymbol{\mathcal{C}}$ and $\boldsymbol{\mathcal{E}}$ [Eqs. (35c) and (35e)] by (the column vector) $\boldsymbol{c}$ and using the stationary condition (17) to obtain

$$\sum_r \mathcal{C}_{kl,r} c_r = \sum_r \mathcal{E}_{k,r} c_r = 0. \tag{39}$$

Therefore one has to require

$$\boldsymbol{\mathcal{C}}^T \delta\tilde{\boldsymbol{\gamma}}^R(0) + \boldsymbol{\mathcal{E}}\,\delta\tilde{\boldsymbol{n}}(0) - \delta\tilde{\boldsymbol{v}}^D(0) = -\boldsymbol{c}\,\delta E(0), \tag{40}$$

where the no-divergence conditions (37) are obeyed for any value of the constant $\delta E(0)$. The constant is not arbitrary but is determined by the choice of the gauge of the applied potential. Suppose the applied potential has a spatially constant part V_0, and the rest of the perturbing potential has diagonal matrix elements zero [as would for instance be the case for a polarizing finite field along the bond axis of H_2, $V(\boldsymbol{r}) = V_0 - \mathcal{E}z$], then $\delta v_{pp}^R(0) = V_0 \forall p$. Multiplying Eq. (40) with $\boldsymbol{c}^T$ and using $\boldsymbol{c}^T\boldsymbol{\mathcal{C}}^T = 0$ and $\boldsymbol{c}^T\boldsymbol{\mathcal{E}} = 0$ and $\delta\tilde{v}_p^D(0) = 2c_p \delta v_{pp}^R(0)$ [Eq. (28b)] leads to

$$\sum_p c_p \delta\tilde{v}_p^D(0) = \sum_p n_p \delta v_{pp}^R(0) = 2V_0 = \sum_p |c_p|^2 \delta E(0) = \delta E(0). \tag{41}$$

So $\delta E(0)$ is simply the shift in energy of this two-electron system with an applied constant field V_0. Of course one can adjust the gauge of the field so that a possible nonzero value of $\Sigma_p n_p \delta v_{pp}^R(0) \equiv 2V_1$ for the rest of the potential is compensated by the choice of gauge, i.e., choose $V_0 = -V_1$ so that $\delta E(0) = 0$. Then condition (40) becomes

$$\boldsymbol{\mathcal{C}}^T \delta\tilde{\boldsymbol{\gamma}}^R(0) + \boldsymbol{\mathcal{E}}\,\delta\tilde{\boldsymbol{n}}(0) = \delta\tilde{\boldsymbol{v}}^D(0). \tag{42}$$

We note that Eq. (40) is equivalent to the perturbed version of Eq. (16) with $\delta\mu = \delta E(0)$. Recovering this equation is crucial for obtaining a correct static response. Equation (16) has its counterpart for a general N-electron system, and indeed this has been perturbed to derive the static response equations of DMFT in Ref. 42. It is important that any approximation recovers Eq. (40) in some way for the $\omega \to 0$ limit. Applying Eq. (42) (also at finite ω) in Eq. (34), which amounts to omitting all terms with ω^{-1} behavior, leads to

$$\omega\,\delta\tilde{\boldsymbol{\gamma}}^R(\omega) + \boldsymbol{\mathcal{A}}\,\delta\tilde{\boldsymbol{\gamma}}^I(\omega) = 0, \tag{43a}$$

$$\boldsymbol{\mathcal{A}}\,\delta\tilde{\boldsymbol{\gamma}}^R(\omega) + \omega\,\delta\tilde{\boldsymbol{\gamma}}^I(\omega) + \boldsymbol{\mathcal{C}}\,\delta\tilde{\boldsymbol{n}}(\omega) = \delta\tilde{\boldsymbol{v}}^R(\omega), \tag{43b}$$

$$\omega\,\delta\tilde{\boldsymbol{n}}(\omega) + \boldsymbol{\mathcal{C}}^T \delta\tilde{\boldsymbol{\gamma}}^I(\omega) = 0, \tag{43c}$$

which looks like an AA in the sense that no ω-dependent coupling matrix elements appear. These equations are actu-

ally practically identical to the equations which have been obtained as the SA in Ref. 26. We will denote them as SA, a comment on the slight difference to the SA of Eq. (3.4) in Ref. 26 can be found in Appendix A.

Excitation energies are obtained in the SA approximation by setting $\delta\tilde{\boldsymbol{v}}^R$ to zero and finding the eigenvalues of

$$\begin{pmatrix} 0 & -\boldsymbol{\mathcal{A}} & 0 \\ -\boldsymbol{\mathcal{A}} & 0 & -\boldsymbol{\mathcal{C}} \\ 0 & -\boldsymbol{\mathcal{C}}^T & 0 \end{pmatrix} \begin{pmatrix} \delta\tilde{\boldsymbol{\gamma}}^R(\omega) \\ \delta\tilde{\boldsymbol{\gamma}}^J(\omega) \\ \delta\tilde{\boldsymbol{n}}(\omega) \end{pmatrix} = \omega \begin{pmatrix} \delta\tilde{\boldsymbol{\gamma}}^R(\omega) \\ \delta\tilde{\boldsymbol{\gamma}}^J(\omega) \\ \delta\tilde{\boldsymbol{n}}(\omega). \end{pmatrix}. \tag{44}$$

Since these equations can also be obtained when one takes in the exact matrix of Eq. (36) the $\omega \to \infty$ limit, the solutions to the SA equations should coincide with the eigenvalues of the exact TDDMFT matrix at $\omega \to \infty$. Figure 4 suggests that at least some eigenvalues will go to zero in the $\omega \to \infty$ limit, possibly those related with diagonal double excitation character. It is in fact possible to deduce that the SA Eq. (44) yield at least m solutions with $\omega=0$ for the excitation energies. We obtain the eigenvalues by setting the secular determinant to zero

$$\begin{vmatrix} \omega\mathbf{1}_M & \boldsymbol{\mathcal{A}} & 0 \\ \boldsymbol{\mathcal{A}} & \omega\mathbf{1}_M & \boldsymbol{\mathcal{C}} \\ 0 & \boldsymbol{\mathcal{C}}^T & \omega\mathbf{1}_m \end{vmatrix} = 0. \tag{45}$$

The determinant of a partitioned matrix can be written

$$\begin{vmatrix} \boldsymbol{A} & \boldsymbol{B} \\ \boldsymbol{C} & \boldsymbol{D} \end{vmatrix} = |\boldsymbol{A}| \cdot |\boldsymbol{D} - \boldsymbol{C}\boldsymbol{A}^{-1}\boldsymbol{B}|, \tag{46}$$

which we use to obtain

$$\begin{vmatrix} \omega\mathbf{1}_M & \boldsymbol{\mathcal{A}} & 0 \\ \boldsymbol{\mathcal{A}} & \omega\mathbf{1}_M & \boldsymbol{\mathcal{C}} \\ 0 & \boldsymbol{\mathcal{C}}^T & \omega\mathbf{1}_m \end{vmatrix} = \omega^m |\omega^2\mathbf{1}_M - \boldsymbol{\mathcal{A}}^2 - \boldsymbol{\mathcal{C}}\boldsymbol{\mathcal{C}}^T|. \tag{47}$$

To find out what causes these m-fold $\omega=0$ roots, we consider the Eq. (43) [no external field, $\delta\tilde{\boldsymbol{v}}^R(\omega)=0$] for $\omega=0$. From Eq. (43a) for $\delta\tilde{\boldsymbol{\gamma}}^R(\omega)$ we obtain $\delta\tilde{\boldsymbol{\gamma}}^J=0$. Equation (43c), $\boldsymbol{\mathcal{C}}^T\delta\tilde{\boldsymbol{\gamma}}^J=0$, is then trivially satisfied so it is redundant. Equation (43b) gives $\boldsymbol{\mathcal{A}}\delta\tilde{\boldsymbol{\gamma}}^R=-\boldsymbol{\mathcal{C}}\delta\tilde{\boldsymbol{n}}$ so we can solve for the M unknowns $\delta\tilde{\boldsymbol{\gamma}}^R$ for a given choice of the vector $\delta\tilde{\boldsymbol{n}}$ as long as $\boldsymbol{\mathcal{A}}$ is invertible. We may choose m independent orthogonal vectors, for instance, $\delta\tilde{n}_k=1$, $\delta\tilde{n}_{l\neq k}=0$ for $k=1,\ldots,m$. So the m $\omega=0$ roots correspond to the m diagonal double excitations, where for each diagonal double excitation the solution of Eq. (43b) determines to what extent single excitations and off-diagonal doubles mix into it. It turns out that such admixture is very small, but not zero. In the present SA approximation the occupation number changes are not strictly zero (as they were in the SA of Ref. 26), but they are (too) small.

An example of the behavior of the double excitations is apparent from the $2\Sigma_g^+$ curve in Fig. 4. The eigenvalue $\epsilon_i(\omega), i=2\Sigma_g^+$ tends to zero for $\omega \to \infty$. This should be true for all the other diagonal double excitations, which numerical solution corroborates. So we will have excitation energies zero for all diagonal double excitations in the SA approximation, which is a serious deficiency of this approximation.

The second factor in the right hand side of Eq. (47) yields M roots for ω^2, corresponding to plus and minus values of ω, i.e., the $2M$ remaining eigenvalues of Eq. (44). Indeed, this second factor is the secular determinant of the equations obtained when substituting for $\delta\tilde{\boldsymbol{\gamma}}^R(\omega)$ and $\delta\tilde{\boldsymbol{n}}(\omega)$ from Eqs. (43a) and (43c) into Eq. (43b),

$$(\omega^2\mathbf{1}_M - \boldsymbol{\mathcal{A}}^2 - \boldsymbol{\mathcal{C}}\boldsymbol{\mathcal{C}}^T)\delta\tilde{\boldsymbol{\gamma}}^J(\omega)/\omega = 0. \tag{48}$$

Evidently, since the secular determinant will have roots in ω^2, the SA equations have preserved the symmetry of the exact TDDMFT equations between positive and negative ω values. Having solved these equations at the eigenvalues ω_i, the full solutions can be obtained by calculating the remaining parts of the eigenvectors of Eq. (44) [the quantities $\delta\tilde{\boldsymbol{\gamma}}^R(\omega_i)$ and $\delta\tilde{\boldsymbol{n}}(\omega_i)$] from $\delta\tilde{\boldsymbol{\gamma}}^J(\omega_i)$ with the Eqs. (43a) and (43c) respectively. This yields M excitation energies (discarding the negative ω values) and excitation vectors, describing the transition densities. The results for the SA calculations to be reported in Sec. VII have been obtained in this way.

Apart from the fact that the SA fails to obtain the excitations with predominant double excitation character, it also fails to reproduce exactly the static polarizability when the response is evaluated for applied fields with $\omega \to 0$, see Ref. 26. The static response of the two-electron system can be obtained independently by perturbing the time-independent stationary conditions [Eqs. (16) and (17)], and has been studied in Ref. 42. As expected this failure persists for general N electron systems.[26] The source of the failure is that the no-divergence conditions (37) are applied in the SA, but they are not included in the set of equations that is solved and therefore are not *enforced*. Actual SA calculations prove that the condition of Eq. (42) does not hold for the solutions obtained.

It is clear that the conditions (42) play a crucial role. We will discuss in the next section attempts to incorporate them. At the end of this section we note that the m zero roots we have found in the SA make it possible to solve this problem of incorporation of 42 straightforwardly in the case of static response ($\omega=0$). The Eq. (42) can simply be added as an additional set of m equations to the exact TDDMFT equations. The $1/\omega$ terms in the first and third sets of equations [Eq. (34a) and Eq. (34c)] can then be eliminated by substitution, enabling solution of the (extended) set of equations at $\omega=0$. The m additional Eq. (42) can be retained, in order to properly enforce them, without the system of equations becoming overcomplete since we saw that the SA equations, which have resulted from the substitution, have a kernel space of dimension m. We can therefore add m equations. Correct static polarization results will be obtained at $\omega=0$. We will consider such polarizability calculations (also at finite ω values, where overcompleteness does occur) elsewhere.

B. Relation with the AA

We note that the approximation indicated as AA in Ref. 26 has also resulted from an attempt to explicitly impose Eq. (42), but in a way which will not solve all deficiencies. In the

AA, Eq. (40) is employed explicitly as one of the equations for the response vector at $\omega=0$. The no-divergence Eq. (37) is then obeyed. When extending the condition to finite ω values, one obtains

$$\boldsymbol{\mathcal{C}}^T\delta\tilde{\boldsymbol{\gamma}}^R(\omega)+\boldsymbol{\mathcal{E}}\delta\tilde{\boldsymbol{n}}(\omega)=\delta\tilde{\boldsymbol{v}}^D(\omega)-\sqrt{2}\boldsymbol{c}\,\delta E(\omega). \tag{49}$$

Application of the condition Eq. (49) should give reasonable results at finite but small ω values, and become exact for $\omega\rightarrow 0$, as required for an AA. In Ref. 26 the m Eq. (49) have not been added but they have been substituted for the third set of the SA equations, the Eqs. (43c) [or rather the Eq. (A1) in that paper]; we shall denote this approximation AA1. With the nondivergence achieved by imposing Eq. (49), we obtain the SA Eq. (43a) from the first exact TDDMFT equation, Eq. (34a). The third of the exact equations, Eq. (34c), would become, with substitution of Eq. (49), the SA Eq. (43c). Now at $\omega=0$ Eq. (43a) gives $\delta\tilde{\boldsymbol{\gamma}}^I(0)=0$ (if $\boldsymbol{\mathcal{A}}$ is invertible). This result when substituted into Eq. (43c) yields the redundant result $0=0$ (at $\omega=0$). This m Eq. (43c) have therefore been discarded in AA1 and have been substituted by the m Eq. (49). This takes care that the no-divergence condition is actually implemented. A set of equations is thus obtained for determining frequency dependent polarizabilities at finite (small) values of ω, that will yield the static polarizability in the $\omega\rightarrow 0$ limit,

$$\omega\delta\tilde{\boldsymbol{\gamma}}^R(\omega)+\boldsymbol{\mathcal{A}}\delta\tilde{\boldsymbol{\gamma}}^I(\omega)=0, \tag{50a}$$

$$\boldsymbol{\mathcal{A}}\delta\tilde{\boldsymbol{\gamma}}^R(\omega)+\omega\delta\tilde{\boldsymbol{\gamma}}^I(\omega)+\boldsymbol{\mathcal{C}}\delta\tilde{\boldsymbol{n}}(\omega)=\delta\tilde{\boldsymbol{v}}^R(\omega), \tag{50b}$$

$$\boldsymbol{\mathcal{C}}^T\delta\tilde{\boldsymbol{\gamma}}^R(\omega)+\boldsymbol{\mathcal{E}}\delta\tilde{\boldsymbol{n}}(\omega)=\delta\tilde{\boldsymbol{v}}^D(\omega)-\sqrt{2}\boldsymbol{c}\,\delta E(\omega). \tag{50c}$$

Specializing now to excitation energy calculations, $\delta\tilde{\boldsymbol{v}}=0$ (hence $\delta E(\omega)=0$], we have to solve $2M+m$ homogeneous equations for $2M+m$ unknowns, which can only be achieved when the determinant of the coefficient matrix is zero,

$$\begin{vmatrix} \omega\mathbf{1}_M & \boldsymbol{\mathcal{A}} & 0 \\ \boldsymbol{\mathcal{A}} & \omega\mathbf{1}_M & \boldsymbol{\mathcal{C}} \\ \boldsymbol{\mathcal{C}}^T & 0 & \boldsymbol{\mathcal{E}} \end{vmatrix}=0. \tag{51}$$

Unfortunately, this yields a characteristic polynomial of only order $2M$ in ω, so only $2M$ roots are obtained. We therefore lose m excitation energies compared to the exact TDDMFT equations. Since the kernel of $\boldsymbol{\mathcal{E}}$ is formed by the vector $\boldsymbol{c}$, the matrix $\boldsymbol{\mathcal{E}}$ can be inverted on a subspace where the vector $\mathbf{c}$ has been projected out. This allows us to write Eq. (50c) as

$$\delta\tilde{\boldsymbol{n}}(\omega)=-\boldsymbol{\mathcal{E}}^{-1}\boldsymbol{\mathcal{C}}^T\delta\tilde{\boldsymbol{\gamma}}^R(\omega). \tag{52}$$

Together with Eq. (50a) one can eliminate $\delta\tilde{\boldsymbol{\gamma}}^R(\omega)$ and $\delta\tilde{\boldsymbol{n}}(\omega)$ from Eq. (50b) to obtain

$$(\omega^2 1_M-\boldsymbol{\mathcal{A}}^2+\boldsymbol{\mathcal{C}}\mathcal{E}^{-1}\boldsymbol{\mathcal{C}}^T\boldsymbol{\mathcal{A}})\delta\tilde{\boldsymbol{\gamma}}^I(\omega)=0. \tag{53}$$

The excitation energies are obtained as the ω_i for which this equation is solvable, i.e., for which the determinant of the matrix of Eq. (53) is equal to zero. From the solution vector $\delta\tilde{\boldsymbol{\gamma}}^I$ the remaining parts, $\delta\tilde{\boldsymbol{\gamma}}^R$ and $\delta\tilde{\boldsymbol{n}}$, are obtained from Eqs. (50a), (50c), and (52). We obviously obtain M ω^2 roots, hence $2M$ symmetrical positive and negative ω_i roots. As with the SA, the symmetry between positive and negative roots has not been lost in AA1. Comparing to the SA equation for the nonzero roots, Eq. (48), the AA1 approximation apparently yields a very similar equation. The calculated excitation energies may not be very different, as will be checked numerically in the next section. More importantly, the AA1 obviously does not solve the problem of the SA of the disappearing (diagonal) double excitations. They are now no longer at $\omega=0$, but they have simply been lost.

The total number of solutions is not the most important issue since from a large basis set many high-lying excitation energies will result, which are not physical. It is, however, important that the m excitations which arise from the $\delta\tilde{\boldsymbol{n}}$ degrees of freedom are properly taken into account. This is important for those states which have significant (diagonal) double excitation character, and it is of course crucial for the "doubly excited" states which have predominantly this character. So we need to retain the third of the exact TDDMFT equations, Eq. (34c) (the "$\delta\tilde{\boldsymbol{n}}$ equation"), it should not be discarded as in AA1 or made inactive as in SA. It is at the same time necessary to build in the nondivergence condition of Eq. (49). It is also clear that, when compared to SA and AA1 we are going to have m additional eigenvalues, up to a total of $2M+m$, so including the m doubly excited states, we no longer can have symmetrical positive and negative roots. If the matrix to be diagonalized is no longer ω-dependent, as was the case for the exact TDDMFT inverse response matrix, we will have not more than $2M+m$ eigenvalues. Our goal can therefore only be to obtain at least $M+m$ positive eigenvalues that constitute (approximations to) the excitation energies. The requirement of obeying the nondivergence condition is met by using as the third set of equations the sum of the third SA equation, Eq. (43c), and the nondivergence condition Eq. (49). We then obtain what we call the AA2 set of equations,

$$\omega\delta\tilde{\boldsymbol{\gamma}}^R(\omega)+\boldsymbol{\mathcal{A}}\delta\tilde{\boldsymbol{\gamma}}^I(\omega)=0, \tag{54a}$$

$$\boldsymbol{\mathcal{A}}\delta\tilde{\boldsymbol{\gamma}}^R(\omega)+\omega\delta\tilde{\boldsymbol{\gamma}}^I(\omega)+\boldsymbol{\mathcal{C}}\delta\tilde{\boldsymbol{n}}(\omega)=\delta\tilde{\boldsymbol{v}}^R(\omega), \tag{54b}$$

$$-\boldsymbol{\mathcal{C}}^T\delta\tilde{\boldsymbol{\gamma}}^R+\boldsymbol{\mathcal{C}}^T\delta\tilde{\boldsymbol{\gamma}}^I(\omega)+(\omega-\boldsymbol{\mathcal{E}})\delta\tilde{\boldsymbol{n}}(\omega)=\sqrt{2}\boldsymbol{c}\,\delta E(\omega)-\delta\tilde{\boldsymbol{v}}^D. \tag{54c}$$

At $\omega=0$ Eq. (54a) [identical to the SA Eq. (43a)] would yield the same result as before ($\delta\tilde{\boldsymbol{\gamma}}^I(0)=0$). However now Eq. (54c) no longer reduces to a redundant $0=0$ equation, but it yields precisely Eq. (49). We therefore have a consistent approximation, since Eq. (49) is enforced at $\omega=0$, which is necessary to make it possible in the first place to remove the ω^{-1} terms of the exact equations and write Eqs. (54a) and (54c) in the above form.

The "AA" AA2 takes fully into account the solutions associated with the $\delta\tilde{\boldsymbol{n}}$ degrees of freedom, and therefore also incorporates changes of occupation number. We obtain m positive eigenvalues corresponding to these excitations. The price we pay for this approximation is loss of symmetry between the other M positive eigenvalues and the M negative eigenvalues. Indeed, it can be proven, from a factorization of the secular determinant of AA2 along the same lines

as the AA1 one in Eq. (47) that with our sign choice for the incorporation of Eq. (49) in order to obtain the proper $\omega \rightarrow 0$ behavior, we obtain meaningful excitation energies from $M+m$ positive (or zero) roots (see Sec. VII). The M remaining negative roots, although they approximately mirror M of the positive roots, need not be meaningful and are discarded. We will deal with just the positive roots, corresponding to positive excitation energies, in all cases (SA, AA1, and AA2).

VII. NUMERICAL RESULTS FOR STRETCHED H_2 AND HeH^+ SYSTEMS

In this section we compare the excitation energies obtained with the various "adiabatic" approximations (i.e., ω-independent coupling matrices) to exact calculations in an aug-cc-pVQZ basis set. The excitation energies can be found by setting $\delta\boldsymbol{v}(\omega)=0$ and searching for ω_i for which the response equations can still be solved (i.e., "free" responses or oscillations can exist in the system). In all cases we have been able to cast this in the form of a straightforward diagonalization. For the calculation of the exact excitation energies, from the linear response equations of the wave function dynamics, we used Eq. (32). For the calculations called SA, the symmetrical matrix of Eq. (48) was diagonalized directly, and the full solutions can then be obtained by calculating the remaining parts of the eigenvectors [the quantities $\delta\tilde{\boldsymbol{\gamma}}^R(\omega_i)$ and $\delta\tilde{\boldsymbol{n}}(\omega_i)$] from $\delta\tilde{\boldsymbol{\gamma}}^I(\omega_i)$ with the Eqs. (43a) and (43c), respectively.

For the AA1 calculations, Eq. (53) is written such that a symmetrical matrix diagonalization can be performed (note that $\boldsymbol{\mathcal{A}}$ and $\boldsymbol{\mathcal{E}}$ are symmetrical matrices),

$$\sqrt{-\boldsymbol{\mathcal{A}}}(\boldsymbol{\mathcal{A}}-\boldsymbol{\mathcal{C}}\boldsymbol{\mathcal{E}}^{-1}\boldsymbol{\mathcal{C}}^T)\sqrt{-\boldsymbol{\mathcal{A}}}\cdot\sqrt{-\boldsymbol{\mathcal{A}}}\frac{\delta\tilde{\boldsymbol{\gamma}}^I(\omega)}{\omega}$$

$$=\omega^2\cdot\sqrt{-\boldsymbol{\mathcal{A}}}\frac{\delta\tilde{\boldsymbol{\gamma}}^I(\omega)}{\omega}. \tag{55}$$

Since the matrix $\boldsymbol{\mathcal{A}}$ is negative semidefinite, the minus sign is required to make the square root well defined. The matrix $\boldsymbol{\mathcal{E}}^{-1}$ is required for the AA1, which is at least singular for one root (the eigenvector $\boldsymbol{c}$ has zero eigenvalue). In the calculations it turned out to be the only singular value and it was simply removed by a standard singular value decomposition. The full solution vector, with $\delta\tilde{\boldsymbol{\gamma}}^R(\omega_i)$ and $\delta\tilde{\boldsymbol{n}}(\omega_i)$ parts, is obtained from Eqs. (50a), (50c), and (52).

For the AA2 model the full matrix of Eq. (54) (with $\delta\tilde{\boldsymbol{v}}=0$) has been diagonalized. Although this matrix is not symmetric, only real eigenvalues were obtained, which can be understood by factorizing the secular determinant of Eq. (54), which with some algebra leads to

$$0=\begin{vmatrix}\omega\mathbf{1}_M & \boldsymbol{\mathcal{A}} & 0\\ \boldsymbol{\mathcal{A}} & \omega\mathbf{1}_M & \boldsymbol{\mathcal{C}}\\ -\boldsymbol{\mathcal{C}}^T & \boldsymbol{\mathcal{C}}^T & \omega 1_m-\boldsymbol{\mathcal{E}}\end{vmatrix}$$

$$=|\boldsymbol{\mathcal{A}}+\omega\mathbf{1}_M|\cdot\begin{vmatrix}\boldsymbol{\mathcal{A}}-\omega\mathbf{1}_M & \boldsymbol{\mathcal{C}}\\ \boldsymbol{\mathcal{C}}^T & \boldsymbol{\mathcal{E}}-\omega\mathbf{1}_m\end{vmatrix}$$

$$=|\boldsymbol{\mathcal{A}}+\omega\mathbf{1}_M|\cdot|\tilde{\boldsymbol{K}}-\omega\mathbf{1}_{M+m}|. \tag{56}$$

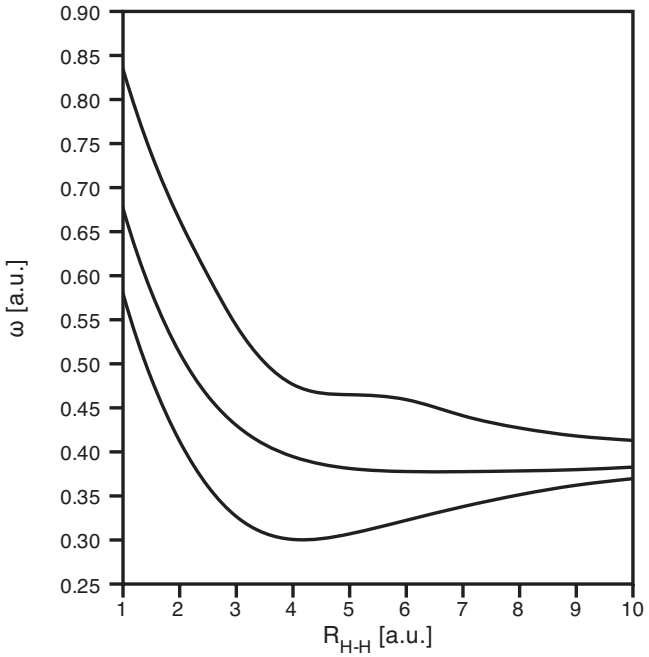

FIG. 6. Plot of Σ_u^+ excitations for dissociating H_2. All AAs coincide with the exact solutions.

It is clear from the hermiticity of $\boldsymbol{\mathcal{A}}$ and $\tilde{\boldsymbol{K}}$ [cf. Eq. (30)] that AA2 has real but different positive and negative solutions. We use the positive excitation energies coming from the factor with the $\tilde{\boldsymbol{K}}$ matrix. Comparing to the equations for the exact wave function dynamics, Eq. (32), it is clear that the AA2 model for the two-electron systems always yields the exact excitation energies.

As a basis set we took the aug-cc-pVQZ (Refs. 34 and 35) basis. The NOs were first obtained with a CISD calculation with the GAMESS-UK[36] package. The integrals in the NO basis were stored on file for the excitation calculation. The expansion coefficients $\boldsymbol{c}$ were calculated within the program using Eq. (14c) directly. For the linear algebra we used the LAPACK routines.[37]

We will discuss the H_2 and HeH^+ systems separately since the symmetry aspects are different. For H_2 we first consider the results for the Σ_u^+ excitations, which are shown in Fig. 6. (The exact results differ from the exact TZP results in the Introduction due to the larger aug-cc-VQZ basis.) Interestingly, in this symmetry the SA, AA1, and AA2 all coincide with the exact excitation energies along the whole bonding distance. This is an effect of the symmetry of these excitations. We first note that all matrices to be diagonalized can be fully symmetry blocked so that we only need to consider the diagonalization per irreducible representation.

Within the Σ_u^+ symmetry, which involves all orbital products kl that are of Σ_u^+ symmetry (or have Σ_u^+ component), the matrix $\boldsymbol{\mathcal{C}}$ is zero since from the definition [Eq. (35c)] it follows that the matrix elements $\mathcal{C}_{kl,r}$ are zero if the NOs k and l involved are of different symmetries. In the first place, then obviously $h_{kl}=0$ (first term of $\boldsymbol{\mathcal{C}}$). Moreover $w_{klrr}=0$ (second term of $\boldsymbol{\mathcal{C}}$) if $\Gamma^k\otimes\Gamma^r$ (density of electron 1) does not contain the same irreducible representation(s) as $\Gamma^l\otimes\Gamma^r$ (density of electron 2), i.e., if

$$A_1 \notin \Gamma^k \otimes \Gamma^r \otimes \Gamma^l \otimes \Gamma^r, \text{ i.e., } A_1 \notin \Gamma^k \otimes \Gamma^l. \quad (57)$$

Now if the pair kl has Σ_u^+ symmetry, i.e., the product of $\Gamma^k \otimes \Gamma^l$ contains Σ_u^+, Γ^k, and Γ^l must be different irreducible representations so their product does not contain $A_1=\Sigma_g^+$ and $w_{klrr}=0$. With a $\boldsymbol{\mathcal{C}}$ matrix equal to zero, Eq. (36) for the exact excitations will have the upper left block of the matrix decoupled from the lower right block (with the $\boldsymbol{\mathcal{E}}^2$ matrix). It is easily seen that the upper left block leads by elimination to the equation $(\boldsymbol{\mathcal{A}}^2-\omega^2 1_M)\delta\tilde{\boldsymbol{\gamma}}^l=0$. However this is precisely also what in the $\boldsymbol{\mathcal{C}}=0$ case the SA of Eq. (48) and the AA1 of Eq. (55) yield. There is no contribution of the $\boldsymbol{\mathcal{E}}^2$ matrix to the Σ_u^+ block since the diagonal double excitations represented by the $\delta\tilde{\boldsymbol{n}}$ never have Σ_u^+ symmetry. Note that these arguments also hold for other excitations such as the Π_g and Π_u excitations.

At the excitation energies (the eigenvalues of $\boldsymbol{\mathcal{A}}^2$) the character of the excitation is determined by the $\delta\tilde{\boldsymbol{\gamma}}^l$, $\delta\tilde{\boldsymbol{\gamma}}^R$ vector ($\delta\tilde{\boldsymbol{\gamma}}^R=\pm\delta\tilde{\boldsymbol{\gamma}}^l$). The lowest Σ_u^+ excited states are all of mostly single excitation type, see Table IV, but off-diagonal doubles also enter. For e.g., the $3\ ^1\Sigma_u^+$, 36% at least are off-diagonal doubles (only 73% of the total composition is shown); for $4\ ^1\Sigma_u^+$ 49% is off-diagonal doubles (72% specified character). The character in terms of NO contributions is therefore very different from the one in TDDFT, which features in this case only $k\leftarrow 1$ $(k\geq 2)$ excitations and no off-diagonal doubles of type $k\leftarrow l$ with $k>l\geq 2$. It would be interesting to perform these calculations in e.g., a KS orbital basis or HF basis instead of NO basis to make a comparison with TDDFT or TDHF possible.

While it is clear now why the SA and AA1 give the same result as the exact calculations since these methods all reduce to diagonalization of $\boldsymbol{\mathcal{A}}^2$, it is also interesting to consider the AA2 model, cf. Eq. (56). In the Σ_u^+ symmetry $\boldsymbol{\mathcal{C}}=0$ and there is no $\boldsymbol{\mathcal{E}}$ block, so AA2 factorizes into $|\boldsymbol{\mathcal{A}}+\omega\mathbf{1}_M|$ and $|\boldsymbol{\mathcal{A}}-\omega\mathbf{1}_M|$ blocks. Obviously, again the same excitation energies (eigenvalues of $\boldsymbol{\mathcal{A}}$) are obtained.

Results for the Σ_g^+ excitations are shown in Fig. 7. Now the energy curves of the AAs are not identical to the exact ones. The SA and AA1 models are completely missing the state with predominantly doubly excited character, that is high lying at short distance and then on its way down crosses the other states, see the dots on the curves indicating the double excited character. For the rest they perform remarkably well, following quite closely the exact curves. The deficiency of the SA and AA1 AAs in TDDMFT, i.e., their inability to represent double excitations, is actually very similar to the adiabatic TDDFT deficiency discussed in Sec. I, except that the agreement of the calculated excitations with the other (nondoubly excited) excitation energies is now much better. The singly excited state $(1\sigma_g\rightarrow 2\sigma_g)$ which is the $2\ ^1\Sigma_g^+$ state (the lowest excited state) below 3 bohr, and which is the second excited state $(3\ ^1\Sigma_g^+)$ at longer bond lengths, is for both the SA and AA1 approximations very accurate compared to the exact calculation. This indicates that the matrix elements of $\boldsymbol{\mathcal{C}}$, although not zero in this symmetry, are still small for this excitation. The coupling of the $\delta\tilde{\boldsymbol{\gamma}}$ to the doubles $\delta\tilde{\boldsymbol{n}}$, which is present in the exact calculation but is absent in the SA and the AA1, is indeed small for this excitation, as is apparent from the small $\delta\tilde{\boldsymbol{n}}$ contributions for the third and higher $^1\Sigma_g^+$ states in Table II. Around 5 bohr the calculated excitation energy deviates somewhat from the exact energy for the $3\ ^1\Sigma_g^+$, although the SA is appreciably better than AA1. At the distance of 5.0 bohr the lack of coupling to diagonal double excitations seems to affect the excitation to the $4\ ^1\Sigma_g^+$ (the highest state in the figure) rather less than it affects the second one. At shorter distance there is clearly the missing of the avoided crossing with the double excitation (around 2.5 bohr).

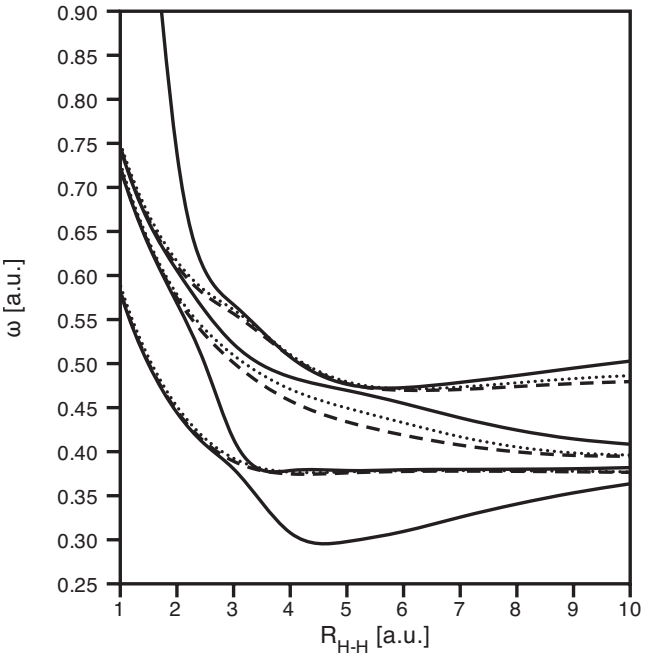

FIG. 7. Plot of Σ_g^+ excitations for dissociating H_2. The exact solutions are represented by the solid lines. The approximated excitation energies are plotted with the dotted and the dashed lines for the SA and AA1, respectively. The AA2 excitation energies coincide with the exact ones.

It is gratifying that the AA2 approximation brings in the coupling to the diagonal doubles very effectively, in fact perfectly. This resolves one of the main disadvantages of SA and AA1, and in fact of adiabatic TDDFT, while still employing an AA in the sense that a constant matrix (ω-independent) can be diagonalized. One does not have to search for ω-roots, as is the case for the exact TDDMFT calculations.

We finally turn to the HeH^+ system, where some of the symmetry advantages of H_2 are lost. The results for the Σ^+ and Π excitations are shown in Figs. 8 and 9, respectively. For the HeH^+ system we observe again that the Π excited states, with a different symmetry than the $^1\Sigma^+$ ground state, are reproduced exactly by all "adiabatic" approximations (see Fig. 9). This good performance of SA and AA1 is possible due to the absence of diagonal double excitation character in the Π states.

It is important to stress that at long distance already some of the lowest of these Π states are pure charge transfer states. The lowest one at 0.810 hartree is for 95% a $He(1s)\rightarrow H(2p_\pi)$ CT transition. The second one at 0.892 hartree, however, is almost purely (97%) a local excitation to $He(2p_\pi)$. Both states are perfectly represented in all the adiabatic calculations.

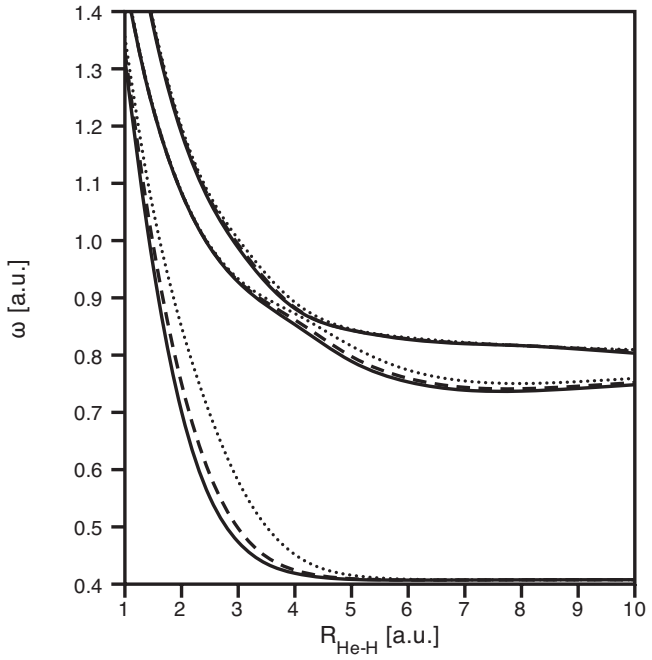

FIG. 8. Plot of Σ^+ excitations for dissociating HeH^+. The exact solutions are represented by the solid lines. The approximated excitation energies are plotted with the dotted and the dashed lines for the SA and AA1, respectively. AA2 coincides with the exact solution.

The low lying Σ^+ excitations are, similar to the Σ_g^+ excitations in H_2, not perfect in the SA and AA1 approximations, but they are clearly rather accurate. In this case the AA1 performs better than the SA, especially for the lowest Σ^+ excitation and also for the other two. We observe that at long distance the lowest excited state, $2\Sigma^+$ at ~ 0.40 hartree, is a pure CT state, $\mathrm{He}(1s) \rightarrow \mathrm{H}(1s)$. On the other hand, $3\Sigma^+$ at ~ 0.74 hartree is at long distance a mixed local ($\mathrm{He}(1s) \rightarrow \mathrm{He}(2s)$) and charge transfer ($\mathrm{He}(1s) \rightarrow \mathrm{H}(2s,2p)$) excitation. The $4\Sigma^+$ at ~ 0.82 hartree is mostly CT, $\mathrm{He}(1s) \rightarrow \mathrm{H}(2s,2p)$. The different characters of these states do not seem to influence the accuracy of the AAs. Diagonal doubles, which will eventually enter states of Σ^+ symmetry, are too high lying to be visible in these figures. For instance, at 8 bohr the first (and rather pure) double is at 2.3 hartree ($\delta\tilde{n}_{60}=0.98$). For those states the SA and AA1 approaches break down. The AA2 is exact for all the Σ^+ (and Π) excited states.

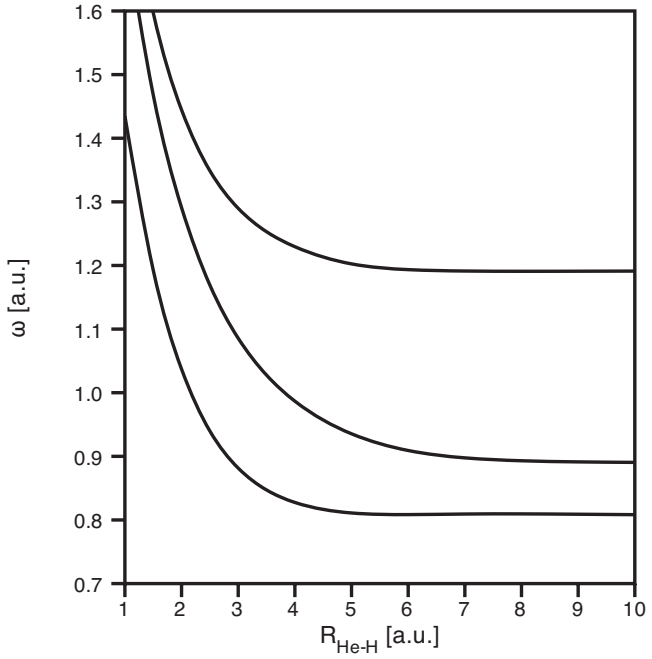

FIG. 9. Plot of Π excitations for dissociating HeH^+. The exact solutions coincides with both approximations.

VIII. CONCLUSIONS

We have studied the time-dependent density matrix method for excitation calculations. In this method the linear response of the one-matrix is used to obtain the excitation energies as the responses ("free oscillations") at zero applied field. Since in two-electron systems the two matrix is known as a functional of the NOs and the NO occupation numbers, one can study the TDDMFT method without the use of approximate functionals. We have shown that the exact TDDMFT equations can then be derived. It provides an exact method for excitation energy calculations, in the sense that its results are identical to those of linear response results for the full wave function dynamics, and indeed to full-CI calculations. It also has exact results for doubly excited configurations, the linear response formalism as such does not restrict the good quality of the results to singly excited states. The exact TDDMFT method has the disadvantage that the excitation energies are not obtained by a single matrix diagonalization, but the matrix is frequency dependent, and an iterative search of excitation energies has to be performed. Approximations are required to obtain an energy-independent matrix, which can be straightforwardly diagonalized. We have been developing such adiabatic approximations. Two simple, previously proposed AAs (SA and AA1) work quite well at the equilibrium distance of the studied systems (H_2 and HeH^+). The agreement is actually perfect for states of different symmetry (irreducible representation) than the totally symmetric ground states. This also holds for two problem cases of TDDFT. The first is exemplified here by the lowest $^1\Sigma_u^+$ excited state of H_2. The PES of this state is totally wrong in TDDFT, going monotonously to zero with increasing R, while it should exhibit a minimum and rise to ca. 10 eV at $R \rightarrow \infty$. The second problem are the charge transfer excitations, which for instance occur in HeH^+ at long bond distance ($\mathrm{He} \rightarrow \mathrm{H}^+$ CT excitations). Also such CT excitations meet with no difficulty in the adiabatic TDDMFT.

For excited states of the same symmetry as the ground state, the situation is different. The approximations SA and AA1 are no longer perfect. They are nevertheless very good at the equilibrium geometry, and also quite decent along the dissociation coordinate for most states. However, a major drawback of SA and AA1 is that states corresponding to doubly excited configurations are totally missed. Also states to which such double excitations make a sizable contribution, are not so accurate. The third adiabatic approximation we have formulated, called AA2, fully incorporates these double excitations. It actually obtains the exact excitation energies (with still an energy-independent matrix, i.e., with a

single diagonalization) in these two-electron systems at the cost that it no longer yields negative energies symmetrical to the positive ones.

We conclude that adiabatic TDDMFT is, in principle, capable of solving the notorious failure cases of TDDFT. TDDMFT in its application on two-electron systems in this paper performs very well. The ultimate applicability of TDDMFT in many-electron systems will depend on the development of DMFT functionals for the exchange and correlation energies in terms of the NOs and occupation numbers. Good progress is being made with such functionals for the ground state, both at equilibrium geometry,[18,22,23,43] as well as along the entire dissociation coordinate,[18,24] which offers good prospects for the response calculations. Reasonable results have been obtained with available functionals such as BBC2 and BBC3 (Ref. 18) for simple diatomics at R_e,[44] but we have found that they do not appear to work well at elongated bond lengths; more development is needed.

APPENDIX A: COMPARISON TO THE SA OF REFERENCE 26

Let us compare the present SA Eq. (43) to the equations which have been introduced as AA (the SA), see Eq. (3.4) in Ref. 26,

$$\omega\delta\tilde{\boldsymbol{\gamma}}^R(\omega)+(\tilde{\boldsymbol{A}}^m)\delta\tilde{\boldsymbol{\gamma}}^I(\omega)=0, \tag{A1a}$$

$$(\tilde{\boldsymbol{A}}^p)\delta\tilde{\boldsymbol{\gamma}}^R(\omega)+\omega\delta\tilde{\boldsymbol{\gamma}}^I(\omega)+\tilde{\boldsymbol{D}}\delta\tilde{\boldsymbol{n}}(\omega)=\delta\tilde{\boldsymbol{v}}^R(\omega), \tag{A1b}$$

$$\omega\delta\tilde{\boldsymbol{n}}(\omega)+2\tilde{\boldsymbol{G}}\delta\tilde{\boldsymbol{\gamma}}^I(\omega)=0, \tag{A1c}$$

where we have defined $\boldsymbol{A}^{p/m}\equiv\boldsymbol{A}\pm\boldsymbol{B}$ and the tilde indicates that we now deal with transformed quantities. The transformation is given by Eq. (33) and note that $\boldsymbol{X}^{R/I}(\omega)=\delta\boldsymbol{\gamma}^{R/I}(\omega)$ and $\boldsymbol{Z}^R(\omega)=\delta\boldsymbol{n}(\omega)$.

These equations are remarkably similar in structure to the Eq. (43). As a matter of fact, if the energy expression Eq. (12) for the two-electron system would be used for the derivations in Ref. 26, the transformations of the two different matrices $\boldsymbol{A}-\boldsymbol{B}$ and $\boldsymbol{A}+\boldsymbol{B}$ would lead to the same matrix $\boldsymbol{\mathcal{A}}=\tilde{\boldsymbol{A}}^m=\tilde{\boldsymbol{A}}^p$, and also $\tilde{\boldsymbol{D}}=\boldsymbol{\mathcal{C}}$ and $2\tilde{\boldsymbol{G}}=\boldsymbol{\mathcal{C}}^T$ would hold. This would imply complete equivalence of our Eq. (43) with the SA Eq. A1 of Ref. 26. However, because as noted before the energy Eq. (12) is not in the form of a proper density matrix functional, it has been rewritten in Ref. 26 in a slightly different form, with the two-electron integrals w_{klkl} being used instead of w_{kkll}. This does not change the stationary total energy, but it has the effect that the energy expression becomes independent of the phases of the NOs, as required for a proper density matrix functional. Using that form of the energy leads to $\tilde{\boldsymbol{A}}^m\neq\tilde{\boldsymbol{A}}^p\neq\boldsymbol{\mathcal{A}}$ and $2\tilde{\boldsymbol{G}}=0$, i.e., to differences with our present equations. These differences turn out to be reasonably small along most of the dissociation coordinate (note, e.g., that the matrix $\boldsymbol{\mathcal{C}}$, although in our case not necessarily zero, is often zero by symmetry anyway, see Sec. VII). Since our present Eq. (43) yields results that are identical to the SA of Ref. 26 if the latter is derived with Eq. (12) for the total energy, and to rather similar results if the SA of Ref. 26 is derived from the alternative energy expression, we have denoted and discussed the approximation incorporated in Eq. (43) in this paper also simply as SA. We will address the subtle issue of the invariance of a proper density matrix functional under the phases of the NOs elsewhere.

APPENDIX B: CHARGE TRANSFER EXCITATIONS OF HeH$^+$ WITH TDDFT

The charge transfer excitation energy in adiabatic TDDFT reduces for two systems that are very far apart (at distances where $1/R$ can be neglected) to just the orbital energy difference between the two orbitals between which the electron transfer takes place since the coupling matrix contribution goes to zero if the differential overlap between donor orbital and acceptor orbital is zero. For the simple example of transfer from the highest occupied molecular orbital (HOMO) of the donor D to the lowest unoccupied orbital (LUMO) of the acceptor A, the excitation energy should be just the difference of ionization energy and electron affinity, $I-A$. Even for a perfect KS calculation, the orbital energy difference between the LUMO of the acceptor and the HOMO of the donor, $\epsilon_A-\epsilon_D$, is in principle not equal to this. Although the exact ϵ_D is equal to $-I$, the exact LUMO energy ϵ_A is not equal to $-A$. Only the energy of the acceptor orbital *in the negative ion* would be equal to $-A$ (since the highest orbital energy is equal to the ionization energy, and the ionization energy of A^- is the electron affinity of A). The orbital energy of the acceptor orbital of A lacking the necessary upshift to its value in A^- leads to the error in the TDDFT excitation energy, which is therefore typically too low.

However, in one case there is no error in the acceptor orbital energy. This is for H^+, where in this zero electron density system both the electron Coulomb potential and the exchange-correlation potential are zero and the orbital energy is simply the normal energy of the $1s$ orbital in the field of the +1 charge of the nucleus. This *is* the electron affinity of this acceptor system. In this particular case the whole error of the TDDFT charge transfer excitation energy in actual calculations arises from the fact that in any generalized gradient approximation (GGA) the donor orbital energy is not equal to the ionization potential, but is too high (not negative enough) by some 4–5 eV. This GGA error is particularly large for the $1s$ orbital energy in He, hence the considerably too low excitation energy in the TDDFT charge transfer calculation in this case. When the systems are at finite distances where $1/R$ is no longer negligible these observations remain true, the He $1s$ orbital energy is shifted down by the field of the proton, and the orbital energy of the H^+ $1s$ LUMO is also shifted down by $-1/R$ because of the $-1/R$ tail in the exact KS potential of the He atom (which, however, is absent in local density approximation or GGA).

APPENDIX C: EXACT TDDMFT WITHIN A TWO-ORBITAL MODEL

To clarify how the nonlinearity in the exact TDDMFT equations introduces additional roots, we evaluate the equations within a two-orbital model. We use a H_2 system with two $1s$ orbitals, one on each H-atom, so the NOs are just $1\sigma_g$

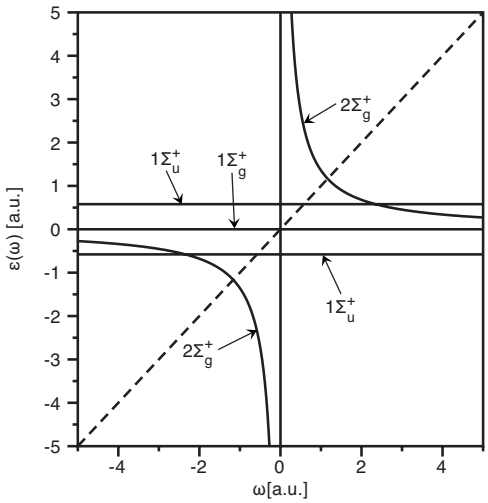

FIG. 10. Plot of $(\chi(\omega))^{-1}$ for H_2 at a bond distance of 5.0 bohr calculated with an STO-6G basis set.

and $1\sigma_u$. We have $m=2$ and $M=1$. Note that we have $\boldsymbol{\mathcal{C}}=0$ since the orbitals belong to different irreducible representations. The secular determinant of Eq. (36) blocks into an upper left part containing $\boldsymbol{\mathcal{A}}$ and a lower left block containing $\boldsymbol{\mathcal{E}}^2$. The first leads to $\epsilon^2-\mathcal{A}_{uggu}^2=0$, corresponding to the Σ_u^+ root

$$\epsilon_{1\Sigma_u^+} = \pm \mathcal{A}_{uggu} = \pm (E_0 - h_{gg} - h_{uu} - w_{uggu} - w_{ugug}). \tag{C1}$$

For the Σ_g^+ roots we have to solve

$$\begin{vmatrix} \epsilon - \dfrac{(\boldsymbol{\mathcal{E}}^2)_{gg}}{\omega} & -\dfrac{(\boldsymbol{\mathcal{E}}^2)_{gu}}{\omega} \\ -\dfrac{(\boldsymbol{\mathcal{E}}^2)_{ug}}{\omega} & \epsilon - \dfrac{(\boldsymbol{\mathcal{E}}^2)_{uu}}{\omega} \end{vmatrix} = 0. \tag{C2}$$

Using the definition of $\boldsymbol{\mathcal{E}}$ we obtain

$$\epsilon_{1\Sigma_g^+} = 0 \quad \text{and} \quad \epsilon_{2\Sigma_g^+} = \frac{4}{n_g n_u} w_{ugug}^2 \frac{1}{\omega}. \tag{C3}$$

In Fig. 10 the solutions are shown as functions of ω in the specific case of H_2 at a distance of 5.0 bohr in a STO-6G basis[45] set.

Although the dimension of the matrix is $m^2=4$, we do obtain $m^2+m=6$ roots from the intersection of the $\varepsilon=\omega$ line with the $\varepsilon_i(\omega)$ curves. The $\varepsilon_{1\Sigma_u^+}$ are constant lines at $\pm\mathcal{A}_{uggu}$, yielding two intersection points. The 2×2 $\boldsymbol{\mathcal{E}}^2$ block yields four roots for the Σ_g^+ symmetry. One is the $\epsilon=0$ root for the ground state. The $\epsilon_{2\Sigma_g^+}$ hyperbola cuts the $\epsilon=\omega$ line at two nonzero points, which are the positive and negative roots corresponding to the $2\Sigma_g^+$ excitation energy. The number of 6 roots is reached by taking into account the intersection of the hyperbola with the $\epsilon=\omega$ line at the "degenerate" $\omega=0$ point, where it switches from $-\infty$ to $+\infty$. In the large basis set calculation on H_2 displayed in Fig. 4 there are also m hyperbolas, but their asymptotes toward $\omega=0$ are not visible, being at too high energy.

[1] E. J. Baerends, Phys. Rev. Lett. **87**, 133004 (2001).
[2] M. Grüning, O. V. Gritsenko, and E. J. Baerends, J. Chem. Phys. **118**, 7183 (2003).
[3] O. Gritsenko, S. J. A. van Gisbergen, A. Görling, and E. J. Baerends, J. Chem. Phys. **113**, 8478 (2000).
[4] K. J. H. Giesbertz and E. J. Baerends, Chem. Phys. Lett. **461**, 338 (2008).
[5] S. Hirata and M. Head-Gordon, Chem. Phys. Lett. **314**, 291 (1999).
[6] C.-P. Hsu, S. Hirata, and M. Head-Gordon, J. Phys. Chem. A **105**, 451 (2001).
[7] D. J. Tozer, R. D. Amos, N. C. Handy, B. O. Roos, and L. Serrano-Andres, Mol. Phys. **97**, 859 (1999).
[8] N. T. Maitra, F. Zhang, R. J. Cave, and K. Burke, J. Chem. Phys. **120**, 5932 (2004).
[9] R. J. Cave, F. Zhang, N. T. Maitra, and K. Burke, Chem. Phys. Lett. **389**, 39 (2004).
[10] J. Neugebauer and E. J. Baerends, J. Chem. Phys. **121**, 6155 (2004).
[11] I. A. Mikhailov, S. Tafur, and A. Masunov, Phys. Rev. A **77**, 012510 (2008).
[12] O. Gritsenko and E. J. Baerends, J. Chem. Phys. **121**, 655 (2004).
[13] A. M. K. Müller, Phys. Lett. **105A**, 446 (1984).
[14] M. Buijse, Ph.D. thesis, Vrije Universiteit, 1991.
[15] M. Buijse and E. J. Baerends, Mol. Phys. **100**, 401 (2002).
[16] C. Kollmar and B. A. Heß, J. Chem. Phys. **120**, 3158 (2004).
[17] C. Kollmar, J. Chem. Phys. **121**, 11581 (2004).
[18] O. V. Gritsenko, K. Pernal, and E. J. Baerends, J. Chem. Phys. **122**, 204102 (2005).
[19] M. Piris, Int. J. Quantum Chem. **106**, 1093 (2006).
[20] M. Piris, X. Lopez, and J. M. Ugalde, J. Chem. Phys. **126**, 214103 (2007).
[21] N. N. Lathiotakis, N. Helbig, and E. K. U. Gross, Phys. Rev. B **75**, 195120 (2007).
[22] N. N. Lathiotakis and M. A. Marques, J. Chem. Phys. **128**, 184103 (2008).
[23] M. A. Marques and N. N. Lathiotakis, Phys. Rev. A **77**, 032509 (2008).
[24] D. R. Rohr, K. Pernal, O. V. Gritsenko, and E. J. Baerends, J. Chem. Phys. **129**, 164105 (2008).
[25] K. Pernal, O. Gritsenko, and E. J. Baerends, Phys. Rev. A **75**, 012506 (2007).
[26] K. Pernal, K. Giesbertz, O. Gritsenko, and E. J. Baerends, J. Chem. Phys. **127**, 214101 (2007).
[27] K. J. H. Giesbertz, E. J. Baerends, and O. V. Gritsenko, Phys. Rev. Lett. **101**, 033004 (2008).
[28] P. Hohenberg and W. Kohn, Phys. Rev. **136**, B864 (1964).
[29] T. L. Gilbert, Phys. Rev. B **12**, 2111 (1975).
[30] E. Runge and E. K. U. Gross, Phys. Rev. Lett. **52**, 997 (1984).
[31] N. N. Bogolyubov, *Problems of Dynamical Theory in Statistical Physics* (OGIZ, Moscow-Leningrad, 1946).
[32] M. Bonitz, *Quantum Kinetic Theory* (Teubner-Verlag, Stuttgart, Leipzig, 1998).
[33] P.-O. Löwdin and H. Shull, Phys. Rev. **101**, 1730 (1956).
[34] T. H. Dunning, Jr., J. Chem. Phys. **90**, 1007 (1989).
[35] D. E. Woon and T. H. Dunning, Jr., J. Chem. Phys. **100**, 2975 (1994).
[36] GAMESS-UK is a package of *ab initio* programs, see: http://www.cfs.dl.ac.uk/gamess-uk/index.shtml; M. F. Guest, I. J. Bush, H. J. J. van Dam, P. Sherwood, J. M. H. Thomas, J. H. van Lenthe, R. W. A. Havenith, and J. Kendrick Mol. Phys. **103**, 719 (2005).
[37] E. Anderson, Z. Bai, C. Bischof, S. Blackford, J. Demmel, J. Dongarra, J. Du Croz, A. Greenbaum, S. Hammarling, A. McKenney, and D. Sorensen, *LAPACK Users' Guide*, 3rd ed.(Society for Industrial and Applied Mathematics, Philadelphia, PA, 1999).
[38] DALTON, a molecular electronic structure program, Release 2.0, 2005, see http://www.kjemi.uio.no/software/dalton/dalton.html.
[39] N. T. Maitra, J. Chem. Phys. **122**, 234104 (2005).
[40] N. T. Maitra, J. Chem. Phys. **125**, 184111 (2006).
[41] M. E. Casida, J. Chem. Phys. **122**, 054111 (2005).
[42] K. Pernal and E. J. Baerends, J. Chem. Phys. **124**, 014102 (2006).
[43] P. Leiva and M. Piris, J. Chem. Phys. **123**, 214102 (2005).
[44] K. Pernal and J. Cioslowski, Phys. Chem. Chem. Phys. **9**, 5956 (2007).
[45] W. J. Hehre, R. F. Stewart, and J. A. Pople, J. Chem. Phys. **51**, 2657 (1969).